

STUDY OF THE MULTI-PORT TECHNOLOGY FOR A MICROWAVE SENSOR APPLICATION

Sandra García Nuño



**Linköping University
INSTITUTE OF TECHNOLOGY**

Department of Science and Technology
Linköping University, SE-601 74 Norrköping, Sweden

Norrköping 2015

ACKNOWLEDGEMENT

My sincerest gratitude goes to my supervisor, Adriana Serban from the University of Linköping. It was a real pleasure to work with her this entire year. I really appreciate the opportunity to carry out this research work in her university, as well as giving me suggestions and feedback. The same words of gratitude go to Ionut Alexandru Apolozan. I really appreciate their guidance, encouragement and support which has been very important in my whole research.

None of this would be possible without my parents, Rafael and Maria José. How far I have come was because of them.

Lastly but certainly not least, I would like to thank my friends Elena and Pelayu. They have always supported me and without them this could not have been done.

CONTEST

ACKNOWLEDGEMENTS.....	2
CONTENTS.....	4
LIST of FIGURES.....	7
LIST of ABBREVIATIONS	10
SPANISH SUMMARY.....	12
1. INTRODUCTION.....	26
1.1 BACKGROUND.....	26
1.2 GOAL and APPROACH.....	28
1.3 OUTLINE of the THESIS.....	29
2. THEORETICAL BACKGROUND.....	31
2.1 INTRODUCTION.....	31
2.2 RECEIVER ARCHITECTURES.....	32
2.3 FREQUENCY-CONVERSION.....	34
2.4 THE MULTI-PORT RECEIVER.....	35
3. HETERODYN RECEIVER MODELLING	39
3.1 TRANSMITTER BLOCK DIAGRAM	41
3.2 RF to IF – PROCESSING BLOCK.....	42
3.3 IF to BASEBAND PROCESSING BLOCK.....	43
3.4 SAMPLING I/Q SIGNALS.....	44
4. PASSIVE COMPONENTS.....	46
BRANCH COUPLER.....	46
<i>THE QUADRATURE (90° HYBRID):.....</i>	<i>46</i>
<i>EVEN-ODD MODE ANALYSIS:.....</i>	<i>47</i>
4.1 SCHEMATIC LEVEL DESIGN in ADS.....	49
4.2 LAYOUT LEVEL DESIGN in ADS.....	51

4.3 S-PARAMETER.....	52
4.4 TRANSIENT SIMULATION.....	55
THE WILKINSON POWER DIVIDER.....	58
<i>EVEN-ODD MODE ANALYSIS:</i>	59
4.5 SCHEMATIC LEVEL DESIGN in ADS.....	62
4.6 LAYOUT LEVEL DESIGN in ADS.....	63
4.7 S-PARAMETERS.....	64
4.8 LAYOUT LEVEL. TRANSIENT SIMULATION.....	67
4.9 TRANSIENT SIMULATION. SIMULATION RESULTS.....	67
<i>ADVANTAGES of USING a WILKINSON POWER:</i>	69
<i>DISADVANTAGES of USING a WILKINSON POWER:</i>	69
5. MULTI-PORT RECEIVER DESIGN.....	70
5.1 LAYOUT LEVEL DESIGN in ADS.....	70
5.2 SCHOTTKY BARRIER DIODE.....	70
5.3 SCHOTTKY BARRIER DIODE CHARACTERISTICS.....	72
5.4 SIMULATION RESULTS.....	75
6. APPLICATION OF MULTI-PORT RECEIVER.....	77
6.1 WIRELESS COMMUNICATIONS SYSTEMS.....	77
6.2 RADAR SYSTEMS.....	78
DOPPLER RADAR.....	79
MULTI-PORT MICROWAVE SENSOR	80
DOPPLER RADAR SIMULATIONS.....	83
7. CONCLUSIONS.....	87
REFERENCES.....	88

LIST of FIGURES

- Figure 1.1 ECG waveform.
- Figure 1.2 Photoplethysmographs.
- Figure 1.3 Heart Sounds.
- Figure 2.1 Real frequency-conversion process.
- Figure 2.2 Examples of Multi-Port network topologies.
- Figure 2.3 Direct conversion (homodyne) receiver architecture.
- Figure 2.4 Heterodyne receiver architecture.
- Figure 2.5 Multi-Port correlator with assigned input signals RF and LO.
- Figure 2.6 Direct conversion Multi-Port receiver using diodes as power detectors.
- Figure 3.1 ADS multiport heterodyne receiver.
- Figure 3.2 ADS transmitter block diagram.
- Figure 3.3 Simulated Results. (a) Ibb signal in ADS, (b) Qbb signal in ADS and (c) RFTxC signal in ADS.
- Figure 3.4 ADS processing block.
- Figure 3.5 Simulated Results. (a) MixInSt1signal in ADS, (b) IFIout signal in ADS and (c) IFIFilt signal in ADS.
- Figure 3.6 IF-BB converter diagram block.
- Figure 3.7 Simulated Results. (a) IFIamp signal in ADS and (b) IBBout signal in ADS. Signal before/after the mixer.
- Figure 3.8 Simulated Results. (a) QBB signal in ADS, (b) Q signal in ADS and (c) I signal in ADS.
- Figure 3.9 Sampling of the final signal.
- Figure 4.1 Geometry of a branch-line coupler.
- Figure 4.2 Descomposition of the branch-line coupler into even-odd mode excitations.
- Figure 4.3 FR4 substrate.
- Figure 4.4 Smart component with S-parameter and Transient parameter simulation set-up.

-
- Figure 4.5 Schematic of the microstrip branch line coupler.
- Figure 4.6 The Branch line coupler as a layout component and simulation set-up.
- Figure 4.7 Simulated S-parameters of the Branch Coupler. (a) S(1,1) parameter, (b) S(1,2) parameter, (c) S(1,3) parameter and (d) S(1,4) parameter.
- Figure 4.8 Simulated S-parameters. S(1,1) , S(1,2), S(1,3), S(1,4).
- Figure 4.9 Optimized parameters.
- Figure 4.10 The Branch line coupler as a layout component and simulation set-up.
- Figure 4.11 Transient Simulation. (a) V_2 , (b) V_3 , (c) V_4 and (d) V_{in} .
- Figure 4.12 Transient Simulation. V_2 , V_3 , V_4 , V_{in} .
- Figure 4.13 Isolation values for several values of n.
- Figure 4.14 (a) An equal-split Wilkinson power divider in microstrip form. (b) Equivalent transmission line circuit.
- Figure 4.15 Frequency response of an equal-split Wilkinson power divider.
- Figure 4.16 Smart component with S-parameter and Transient parameter simulation set-up.
- Figure 4.17 Schematic of the microstrip Wilkinson power divider.
- Figure 4.18 The Wilkinson power divider as a layout component S-parameters simulation set-up.
- Figure 4.19 Simulated S-parameters of the Wilkinson Power Divider .(a) S(1,1), (b) S(1,2) and (c) S(1,3) parameter.
- Figure 4.20 Simulated S-parameter. S(1,1) ,S(1,2) and S(1,3) parameter.
- Figure 4.21 Optimized parameters.
- Figure 4.22 The Wilkinson power divider as a layout component and transient simulation set-up.
- Figure 4.23 Transient Simulation. (a) V_2 , (b) V_3 , and (c) V_{in} .
- Figure 4.24 Transient Simulation. V_2 , V_3 , V_{in} .
- Figure 5.1 Schematic of the Multi-Port heterodyne receiver.
- Figure 5.2 Diode HSMS286x definition.
- Figure 5.3 Schematic of diode HSMS286x.
-

Figure 5.4 Symbol of diode HSMS286x.

Figure 5.5 Simulation set-up of the ideal Multi-Port receiver.

Figure 5.6 Simulation set-up of the Multi-Port receiver.

Figure 5.7 Demodulation results.

Figure 6.1 A basic radio system.

Figure 6.2 Doppler radar system.

Figure 6.3 Doppler Effects.

Figure 6.4 Multi-port microwave sensor with direct conversion architecture.

Figure 6.5 Doppler radar implements in ADS – behavioral level.

Figure 6.6 Target model in ADS for a Doppler radar.

Figure 6.7 Simulation Results. (a) TPA_Baseband_Spectrum, (b)
TPB_Carrier_Spectrum.

Figure 6.8 Simulation ADS for a Doppler-radar.

Figure 6.9 Simulation ADS for a Doppler-radar.

LIST of ABBREVIATIONS

Symbol	Definition
ADS	Advanced Design System
BLC	Branch-Line Coupler
BPF	Band-Pass Filter
LO	Local Oscillator
LNA	Low-Noise Amplifier
LNB	Low-Noise Block
LND	Low-Noise Downconverter
FR4	Standard PCB
HD	High Definition
I/Q	In-phase/Quadrature
IF	Intermediate Frequency
NF	Noise Figure
MLIN	Microstrip Line
MCORN	90° Microstrip Bend
RF	Radio Frequency
PCB	Printed Circuit Board
QBLC	Quadrature Branch Line Coupler
QPSK	Quadrature Phase-Shift Keying
VHF	Very High Frequency
WPD	Wilkinson Power Divider

SPANISH SUMMARY

1. INTRODUCCIÓN

Hoy en día la tecnología médica es utilizada para salvar vidas. Se utiliza a la hora de diagnosticar, monitorizar y tratar cada enfermedad ó afección de los pacientes. El punto en común que tienen todas las aplicaciones en la tecnología médica es el impacto beneficioso sobre la salud y el incremento de la calidad de vida. Todo ello contribuye a vivir más tiempo y mejorar nuestra calidad de vida, entre otras muchas cosas.

La frecuencia cardíaca es uno de los parámetros más medidos frecuentemente por el ser humano. Desempeña un papel importante en la determinación de la salud de un individuo.

La medición de la frecuencia cardíaca se está convirtiendo en una parte del estilo de vida del ser humano, y muchos dispositivos electrónicos, como iPods, equipos de ejercicios y teléfonos móviles, son capaces de medirla con gran precisión.

1.1 ANTECEDENTES

Éste proyecto se realizó dentro del grupo de investigación de *Comunicaciones Electrónicas* en la Universidad de Linköping (Suecia) como parte de un proyecto de investigación que comenzó en otoño de 2015.

Existen varios métodos utilizados para medir la frecuencia cardíaca tales como el electrocardiografía, fotopletismografía, oscilometría y fonocardiografía. Cada uno de ellos mide diferentes fenómenos que se producen en el cuerpo humano durante el latido del corazón ó durante el ciclo cardíaco. Vamos a hacer un breve resumen de cada uno de ellos.

Electrocardiografía: La contracción y relajación de los músculos cardiacos hace que la sangre fluya dentro y fuera del corazón. Durante cada ciclo cardíaco, un grupo de tejido en el corazón llamado nódulo auricular genera impulsos eléctricos que se propagan a través de él y provocan la contracción rítmica y la relajación de los músculos cardíacos.

Estos impulsos eléctricos pueden detectarse colocando electrodos en puntos específicos del cuerpo humano. Un electrocardiograma capta este impulso eléctrico variable.

Fonocardiografía: La apertura y cierre de las válvulas en el corazón produce sonidos durante la contracción y la dilatación, que normalmente es audible a través de un estetoscopio. Estos sonidos son rítmicos al latido del corazón y pueden ser detectados usando micrófonos. Los sonidos cardíacos normalmente se utilizan para determinar la frecuencia cardíaca. Con un filtrado adecuado se pueden visualizar las anomalías del corazón.

1.2 OBJETIVO

El objetivo de este proyecto es analizar y diseñar un receptor cuasi-pasivo multipuerto. El diseño se realizará mediante un programa llamado Advanced Design System (ADS). Este trabajo incluye la implementación en ADS de un receptor de radio heterodino y analizará la posibilidad de la aplicación del receptor multipuerto para aplicaciones de radar. Un radar monostático con tecnología de conversión directa multipuerto será considerado para el latido del corazón y la detección de la respiración.

1.3 DESCRIPCIÓN DEL PROYECTO

Este proyecto consta de 5 capítulos, todos ellos se discuten de forma independiente.

Capítulo 1: Introducción - El primer capítulo es una breve introducción a este proyecto. Da una visión general sobre el informe y el trabajo de éste.

Capítulo 2: Antecedentes teóricos - El segundo capítulo trata sobre el fondo teórico de este proyecto. Se presenta un breve resumen de las arquitecturas de receptor tradicionales e introduce el receptor multipuerto. El comportamiento del correlador multipuerto se analiza utilizando un modelo matemático.

Capítulo 3: Modelado de un receptor heterodino - Presenta un modelo de referencia de un receptor heterodino en ADS.

Capítulo 4: Componentes Pasivos - Introduce la teoría básica de los componentes pasivos de microondas, es decir, el acoplador de línea de derivación en cuadratura y el divisor de potencia Wilkinson.

Capítulo 5: Diseño del receptor multi-puerto - El quinto capítulo presenta el diseño del correlador y receptor multipuerto, que es modelado y simulado en ADS usando componentes reales.

Capítulo 6: Sensor de microondas multi-puerto - En el sexto capítulo, se analiza el uso del receptor multipuerto como un sensor de microondas.

Capítulo 7: Conclusiones - El séptimo capítulo resume y concluye el proyecto.

2. ANTECEDENTES TEÓRICOS

En este capítulo se presenta la teoría básica relacionada con este proyecto. Mostrando especial atención a las arquitecturas tradicionales del receptor seguido de una introducción al receptor multipuerto.

2.1 INTRODUCCIÓN

Los terminales de radio configurables requieren receptores capaces de soportar tantos servicios como sea posible en diferentes frecuencias de operación. En este aspecto, las arquitecturas de receptores clásicos están diseñados para esquemas de modulación y demodulación específicos y siguiendo ciertos estándares de comunicación. Sin embargo, se han introducido otras arquitecturas, como el receptor de seis puertos.

La técnica del receptor de seis puertos fué introducida por primera vez en los años 1960 y 1970 para realizar mediciones de microondas.

Los receptores heterodinos convencionales requieren filtros en RF e IF, que normalmente sólo pueden ser implementados por filtros de onda acústica ó filtros de cristal. Por lo tanto, no se puede lograr una integración en un único chip de pequeño tamaño y bajo coste. Por esa razón, los diseñadores han estado dirigiendo sus esfuerzos hacia el receptor homodino, mejor conocido como el receptor de conversión directa. El

receptor de conversión directa es particularmente conocido, sobretodo dentro de la comunidad investigadora. Existen muchos problemas debido a las deficiencias analógicas cuando se implementa un receptor de conversión directa. Por lo tanto, se buscan otras arquitecturas para el receptor. Una de las arquitecturas más prometedoras es la multipuerto.

Además, siempre hay un cierto misterio al respecto. Algunas publicaciones lo llaman "Caja negra con dos entradas y cuatro salidas". Los puertos de salida terminan con detectores de potencia.

2.2 ARQUITECTURA DEL RECEPTOR

El extremo frontal de RF es el término que recibe a la etapa que va comprendida desde la antena hasta la etapa del mezclador. Lo constituyen todos los componentes del receptor que procesan la señal en la frecuencia de radio entrante original (RF), antes de convertirla a una frecuencia intermedia inferior ó a banda base. Esta conversión de la señal RF se puede realizar en uno ó varios pasos. Dependiendo de esto, se pueden distinguir dos tipos de arquitectura de receptores, pudiendo ser receptor homodino ó receptor heterodino. En el receptor homodino, la frecuencia portadora es igual a la frecuencia de la señal LO a la entrada del mezclador. Si por el contrario las frecuencias RF y LO1 son diferentes, el receptor se llama heterodino.

2.3 CONVERSIÓN DE FRECUENCIAS

La conversión de frecuencia es el proceso de desplazamiento del espectro de una señal. Existen varias razones para realizar dicha conversión. Cuando se quiere conseguir una separación de un cierto número de señales en un medio de transmisión ó para poder emitir una señal por una antena.

2.4 RECEPTOR MULTIPUERTO

El receptor multipuerto consiste en un correlador multipuerto junto con varios componentes tales como diodos ó transistores, usados para realizar la detección de

potencia y así completar el proceso de conversión descendente de frecuencia portadora a frecuencia IF ó frecuencia de banda base.

El correlador multipuerto consiste en un divisor de potencia llamado Wilkinson (WPD) junto con tres acopladores QBLC. Son estructuras pasivas que utilizan la propiedad de las líneas de transmisión $\lambda/4$ para retrasar las señales entrantes con una diferencia de fase precisa, es decir, 90° . Además, cuando se utilizan dos señales de entrada, se produce una superposición de dichas señales.

3. MODELO DEL RECEPTOR HETERODINO

El uso de la simulación para diseñar sistemas eléctricos y componentes no sólo tiene un significado práctico, sino que también es necesario a medida que aumenta la complejidad de los sistemas de comunicación. Diseñar y optimizar estos sistemas y componentes a menudo requiere de una buena comprensión de los sistemas y de los parámetros y variables que influyen en el rendimiento del sistema. La simulación permite al diseñador tener en cuenta estas variables en un único entorno y ayuda a reducir el tiempo de diseño del sistema.

En este capítulo se realizará la implementación y simulación de un receptor heterodino. Este receptor no hará uso de circuitos del mundo real. Luego, en los próximos capítulos, se implementará un receptor multipuerto homodino. En este caso, los circuitos principales del receptor se diseñarán utilizando componentes del mundo real.

La señal recibida en dicho circuito es una señal modulada RF QPSK. Las simulaciones se realizarán utilizando una frecuencia portadora de 60 GHz y la FI del receptor heterodino a 900 MHz.

3.1 DIAGRAMA DEL BLOQUE DEL TRANSMISOR

Las simulaciones se realizan utilizando una frecuencia portadora de 60 GHz, se eligió la IF del receptor heterodino a 900 MHz para obtener una señal QPSK. Se utiliza una

señal QPSK de 100 Mbps generada en el transmisor de señal con dos generadores de datos en banda base conectados al bloque modulador I/Q.

3.2 BLOQUE DE PROCESAMIENTO

La etapa RF contiene un amplificador, varios mezcladores, un filtro BPF Butterworth y un mezclador I/Q.

3.3 BLOQUE DE PROCESAMIENTO BANDA BASE

Los componentes I/Q se amplifican y se transmiten a través de un mezclador obteniendo las dos señales de banda base IBBout y QBBout.

3.4 MUESTREO DE SEÑALES I / Q

En este paso se produce la conversión analógica a digital de las señales en banda base.

4. COMPONENTES PASIVOS

En este capítulo se introduce la teoría básica de los componentes pasivos de microondas, es decir, el acoplador en cuadratura y el divisor de potencia Wilkinson.

ACOPLADORES

Los acopladores direccionales pueden ser de muchas formas. Son circuitos de cuatro puertos donde existe un puerto que está aislado con respecto al puerto de entrada. Todos los puertos están emparejados, y el circuito es sin pérdidas. La mayoría de las veces, se usan para muestrear una señal. Normalmente utilizan propiedades de circuitos de microondas.

HÍBRIDO 90°

El híbrido de 90° es un dispositivo de 4 puertos, conocido como acoplador de cuadratura ó acoplador de línea de derivación. Tienen una diferencia de fase de 90° entre salidas. Se utiliza en microstrip y stripline. Otros acopladores de 3 dB también pueden funcionar como un acopladores en cuadratura.

Funciona de la siguiente manera, la potencia pasa por el puerto 1 y se divide en los puertos 2 y 3, con un cambio de fase de 90º entre estas salidas. No hay alimentación por el puerto 4 (puerto aislado).

Se puede observar que el híbrido tiene un alto grado de simetría, ya que cualquier puerto se puede utilizar como puerto de entrada. Los puertos de salida estarán siempre en el lado opuesto de la unión desde el puerto de entrada, y el puerto aislado será el puerto restante en el mismo lado que el puerto de entrada. Esta simetría se refleja en la matriz de dispersión, ya que cada fila se puede obtener como una transposición de la primera fila.

ANÁLISIS PAR-IMPAR

Trabajamos con el circuito esquemático de un acoplador de línea en forma normalizada. Cada línea representa una línea de transmisión con impedancia característica normalizada a Z_0 . El circuito puede descomponerse mediante la superposición de modo par y de modo impar. Dado que el circuito es lineal, la respuesta real puede obtenerse a partir de la suma de las respuestas del modo par e impar.

4.1 DISEÑO NIVEL ESQUEMÁTICO en ADS

En primer lugar, se define el sustrato de PCB. Dicho sustrato será utilizado durante toda la tesis. Se trabajará a una frecuencia central específica, en este caso, 2,5 GHz. Se ha creado una variable llamada f_0 para este valor. La respuesta en frecuencia del circuito se elegirá para +/- 1GHz. La simulación en el dominio del tiempo tiene un StopTime de 3.5 nsec y un step-size máximo de 10 nsec.

El sustrato FR4 tiene una permitividad relativa (ϵ_r) de 4,6, tiene 0 mm de rugosidad y una permeabilidad relativa (μ_r) de 1 (material no magnético). El coeficiente de acoplamiento indica la relación que existe entre la potencia de entrada y la potencia acoplada.

4.2 NIVEL DE DISEÑO en ADS

Momentum, es una parte del program ADS que permite generar simulaciones de parámetros S para circuitos como stripline, etc... Debemos seleccionar un "plan de frecuencia" en el ADS. En primer lugar, establecimos el tipo "Adaptativo" de frecuencia y se decidió tomar 1.5 GHz como Fstart y 3.5 GHz como Fstop y finalmente Npts -40.

4.3 PARÁMETROS S

Son comunes para redes que operan a frecuencias de radiofrecuencia (RF) y microondas. Son analíticamente convenientes y capaces de proporcionar una gran comprensión de un problema de medición ó diseño. El coeficiente de acoplamiento debe ser positivo y superior a 3 dB. Analizando los resultados obtenidos en el proyecto observamos que el acoplador de ramificación funciona mejor a 2,5 GHz, donde S (1,1) = -22 dB. Además, a 2,1 GHz no irradiará prácticamente nada, ya que S (1,1) es cercano a 0 dB (por lo que toda la potencia se refleja). Si el ancho de banda se define como el rango de frecuencias en el que S (1,1) debe ser inferior a -5 dB, entonces el ancho de banda sería aproximadamente 0,5 GHz, con 2,3 GHz en el extremo superior y 2,8 GHz en el extremo inferior de la banda de frecuencias.

4.4 RÉGIMEN TRANSITORIO

Las simulaciones para el régimen transitorio sólo pueden realizarse cuando se aplica una señal de dominio temporal, por ejemplo, onda senoidal. Por lo tanto, se necesita una fuente P_1Tone en el puerto 1. Se eligió una $Z = 50 \Omega$ y una frecuencia a 2,5 GHz. Los resultados fueron optimizados para la frecuencia dada.

Es análisis siempre comienza en el instante = 0 y asume que sólo las fuentes de CC estaban conectadas al circuito en ese momento. El análisis transitorio ahorra voltajes de nodo y corrientes de derivación en cada punto de tiempo en el análisis. Los pasos de menor duración en el análisis transitorio mejoran la precisión de la medición.

DIVISOR DE POTENCIA WILKINSON

Los puertos de salida están emparejados, sólo la energía reflejada se disipa. Sus puertos de salida están aislados. En este tipo de divisores, hay cuatro secciones diferentes. Puerto de entrada, transformadores $\lambda/4$, resistencias de aislamiento y puertos de salida. Los puertos de entrada y salida son idénticos y el valor de las impedancias de los mismos es Z_0 .

Uno de los mayores inconvenientes del divisor de potencia Wilkinson es que tiene un ancho de banda bastante estrecho. Esto se puede mejorar añadiendo una sección de longitud $\lambda/4$ delante del combinador de potencia. De esta manera, la transformación de impedancia se realiza en dos etapas, mejorando así el ancho de banda. El ancho de banda del divisor de potencia también puede aumentarse dividiendo las secciones de longitud de onda en secciones múltiples con una resistencia entre cada sección.

VENTAJAS DEL USO DE UN DIVIDOR DE POTENCIA WILKINSON:

Simplicidad: El divisor de potencia Wilkinson es simple y se puede hacer fácilmente usando componentes en una placa de circuito impreso. También es posible utilizar elementos inductores y capacitores agrupados, pero esto complica el diseño general.

Coste: Cuando el divisor de potencia Wilkinson se hace usando elementos de circuito impreso, el coste es muy bajo.

Pérdida: Si se usan componentes perfectos, el divisor de potencia Wilkinson no introduciría ningún pérdida adicional entre los diferentes puertos. Además de esto, los componentes reales usados para el divisor de potencia pueden tener pérdidas muy bajas.

Aislamiento: El divisor Wilkinson proporciona un alto grado de aislamiento entre los puertos de salida.

DESVENTAJAS DEL USO DE UN PODER DE WILKINSON:

Respuesta de frecuencia: Como el divisor de potencia se basa en el uso de líneas de transmisión $\lambda/4$, tiene un ancho de banda limitado.

5. DISEÑO DEL RECEPTOR MULTIPUERTO

En este capítulo se presenta el diseño del correlador multipuerto y la simulación en ADS.

5.1 NIVEL DE DISEÑO en ADS

En el diseño combinamos tres acopladores con un divisor de potencia Wilkinson. Tenemos dos entradas y 6 salidas. Conectamos el divisor de potencia Wilkinson como la entrada principal y las 6 salidas procederán de los tres acopladores. Así, los enlazamos con MLIN (Línea Microstrip). También agregamos un MLIN en el Puerto "P1". MLIN (línea Microstrip) se construyó sobre un sustrato FR4 (PCB estándar).

5.2 DIODO DE BARRERA SCHOTTKY

Utilizaremos un diodo Schottky HSMS-286x. Es una familia de diodos detectores polarizados que han sido diseñados y optimizados para el uso frecuencias entre 915 MHz a 5.8 GHz. Son ideales para RF/ID y aplicaciones de RF, así como para la detección de señales, modulación y conversión de RF a DC. A continuación podemos ver las características del diodo que vamos a utilizar. Tiene diferentes configuraciones.

Esto decide el rango dinámico de los detectores de diodos y por lo tanto el rango dinámico de todo el sistema receptor.

5.3 CARACTERÍSTICAS DEL DIODO DE BARRERA SCHOTTKY

Un diodo de barrera Schottky consiste en un metal semiconductor formado por una capa de metal sobre un semiconductor. Es un diodo semiconductor con una baja caída de tensión directa y una acción de conmutación muy rápida.

Todas las curvas de diodos Schottky tienen la misma pendiente, pero no necesariamente el mismo valor de corriente para un voltaje dado. Esto es debido a la corriente de saturación, I_S , y está relacionado con la altura de la barrera del diodo.

A través de la elección de silicio de tipo p ó silicio de tipo n, y la selección de metal, se puede indicar las características de un diodo Schottky. Generalmente, sólo los diodos de

barrera baja se realizan sobre silicio de tipo p. La elección de la combinación del metal y del semiconductor determina la tensión directa del diodo. Tanto el tipo n como el tipo p.

6. APLICACIÓN DEL RECEPTOR MULTIPUERTO

En este capítulo se analiza el uso del receptor multipuerto mediante un sensor de microondas para la detección de signos vitales.

6.1 SISTEMAS DE COMUNICACIONES INALÁMBRICAS

Las comunicaciones inalámbricas son, el segmento de más rápido crecimiento de la industria de las comunicaciones. Los sistemas celulares han experimentado un crecimiento exponencial durante la última década y actualmente hay alrededor de dos mil millones de usuarios en todo el mundo. Muchas nuevas aplicaciones, incluidas redes de sensores inalámbricos, automóviles y fábricas automatizadas, aparatos y telemedicina remota, están siendo investigados hoy en día. Muchos desafíos técnicos permanecen en el diseño de redes inalámbricas robustas que ofrecen el rendimiento necesario para soportar las aplicaciones emergentes, como el sensor de radar para la respiración y la monitorización del latido.

La visión de las comunicaciones inalámbricas que apoyan el intercambio de información entre personas y dispositivos es la frontera de las comunicaciones de las próximas décadas. Los sensores inalámbricos tienen una enorme gama de aplicaciones tanto comerciales como militares. En nuestro caso de estudio, nos centraremos en la comunicación entre un dispositivo y un paciente en el que la señal radiada del dispositivo, se refleja principalmente en la capa superior de la piel del paciente.

El crecimiento exponencial del uso del teléfono móvil y el acceso inalámbrico a Internet han generado un gran optimismo sobre la tecnología inalámbrica en general. Obviamente no todas las aplicaciones inalámbricas florecerán. Mientras que muchos sistemas inalámbricos y empresas han disfrutado de un éxito espectacular, ha habido

muchos fallos en el camino. De hecho, es imposible predecir qué problemas y triunfos inalámbricos se encuentran en el horizonte. Además, debe haber suficiente flexibilidad y creatividad entre los ingenieros. Los sistemas inalámbricos actuales y emergentes de hoy y la visión de aplicaciones que la tecnología inalámbrica puede permitir asegurar un futuro brillante para la tecnología inalámbrica

6.2 SISTEMAS DE RADAR

Una de las aplicaciones más frecuentes de la tecnología de microondas es la radio detección. En su funcionamiento básico, un transmisor envía una señal que es parcialmente reflejada por un objetivo alejado, y luego detectada por un receptor sensible. La distancia al objetivo se determina por el tiempo requerido para que la señal viaje al objetivo y vuelva.

Los primeros trabajos de radar se producieron en Estados Unidos y Gran Bretaña comenzando en la década de 1930, usando fuentes de frecuencia muy alta (VHF). Un gran avance se produjo a principios de 1940. Las frecuencias más altas permitieron el uso de antenas de tamaño razonable con alta ganancia, permitiendo el seguimiento mecánico de blancos con buena resolución angular.

La mayoría de los radares son de tipo monostático, pero en algunas aplicaciones el objetivo es iluminado por una antena de transmisión. A veces se utilizan antenas separadas para lograr el aislamiento necesario entre el transmisor y el receptor. Se supone que el objetivo está en la dirección del haz principal de la antena. El objetivo es dispersar el incidente.

EFFECTO DOPPLER

El efecto Doppler se observa cada vez que la fuente de las ondas se mueve con respecto a un observador. El efecto Doppler se puede describir como el efecto producido por una fuente móvil de ondas en la que hay un aparente cambio ascendente de frecuencia para los observadores hacia los que se aproxima la fuente. Es importante notar que el efecto no se debe a un cambio real en la frecuencia de la fuente. El efecto Doppler se puede observar para cualquier tipo de ola - onda de agua, onda sonora, onda de luz, etc

Estamos más familiarizados con el efecto Doppler debido a nuestras experiencias con las ondas de sonido.

SENSOR DE MICROONDAS MULTIPUERTO

El sistema de radar utilizado en esta aplicación utiliza ondas continuas moduladas en frecuencia que se transmiten al aire libre mediante el uso de una antena. La señal radiada se reflejará en la capa superior de la piel del paciente, se dirigirá de nuevo al sistema y se recibirá a través de la misma antena, que se han enviado. Esta onda está siendo procesada por un correlador multipuerto y varios detectores de potencia. Este sistema multipuerto funciona como un interferómetro, sus señales de salida son combinaciones lineales de señales de entrada desplazadas en fase. Como resultado, la información puede ser extraída por la ola que fue enviada previamente. Sus puntos más importantes son, la discriminación de fase, procesamiento de la señal, complejidad baja del circuito, operación de banda ancha, tarifa de datos alta y coste.

Como se mostró en el capítulo 2, el latido del corazón y las actividades de respiración afectan a la fase de la señal reflejada, que se compara con la fuente de la señal de referencia en el dispositivo de radar. La señal radiada se reflejará principalmente en la capa superior de la piel del paciente, entonces, la respiración del paciente dará como resultado un movimiento periódico del "objetivo" en el intervalo de varios milímetros. Finalmente, el latido del corazón se superpondrá a este movimiento y estará en un rango inferior al milímetro.

7. CONCLUSIONES

Basándose en los conocidos antecedentes de la técnica multipuerto, los resultados de demolición demuestran la validez de la arquitectura heterodina propuesta para el sensor de radar multipuerto.

Si la diferencia entre el portador y el oscilador local no es exactamente igual a IF, la constelación demodulada gira en el sentido de las agujas del reloj ó antihorario

dependiendo del signo de esta diferencia. El rango dinámico se ha logrado gracias al uso de diodos detectores polarizados.

Los resultados revelan la teoría básica sobre los receptores multipuerto (arquitectura multipuerto ha sido implementado para 2,5 GHz). Se ha demostrado que el sexto puerto ofrece la posibilidad de realizar un receptor de banda ancha. La comparación con las arquitecturas de receptores convencionales mostró que el receptor multipuerto es una interesante alternativa a las arquitecturas basadas en mezcladores existentes, especialmente en la gama de ondas milimétricas y sub milimétricas.

Se demostró empíricamente y cuantitativamente el comportamiento multibanda de la arquitectura multipuerto y la capacidad de realizar altas velocidades de datos. La ventaja principal de la arquitectura multipuerto es su ancho de banda extremadamente grande, que implica capacidades multi-banda y multi-modo. Sin embargo, un problema importante es las grandes dimensiones de la estructura pasiva de multipuerto. Como sabemos, el sistema receptor multipunto no requiere suministro de polarización externa y el requisito de potencia LO es comparable al nivel de potencia RF. Estos resultados pueden llevar a considerar la arquitectura multipuerto como una alternativa para aplicaciones de comunicación móvil.

1. INTRODUCTION

Medical technology can be considered as any technology used to save lives in people suffering from a wide range of conditions. In its many forms, medical technology is already diagnosing, monitoring and treating virtually every disease or condition that affects us. The common thread through all applications of medical technology is the beneficial impact on health and quality of life. They all contribute to living longer, better and empowering citizens to contribute to society for longer. They improve the quality of care, and the efficacy and sustainability of healthcare systems [1].

Heart rate is one of the most frequently measured parameters of the human body and plays an important role in determining an individual's health. Heart rate measurement is becoming a part of the typical consumer lifestyle, and many electronic devices such as iPods, exercise equipment, and mobile phones are becoming able to accurately measure heart rate. This functionality, however, does not come without added cost. By using multifunctional devices, developers can reduce the price of introducing new features such as these.

1.1 BACKGROUND

This degree Thesis was performed within the research group Communications Electronics at Linköping University as a part of a research project that will start in autumn of 2015.

Various methods used to measure heart rate include Electrocardiography, Photoplethysmography, Oscillometry and Phonocardiography. Each of these methods measures different phenomenon that occur in human body during the heart beat or cardiac cycle to determine heart rate [2].

Electrocardiography: The contraction and relaxation of cardiac muscles causes blood to flow in and out of the heart. During each cardiac cycle, a group of tissue in the

heart called the sino atrial node generates electrical impulses that spread all through the heart and cause rhythmic contraction and relaxation of heart muscles. These electrical impulses can be detected by placing electrodes in specific points in human body. An electrocardiogram (ECG) captures this varying electrical impulse so shows the overall rhythm of the heart [2].

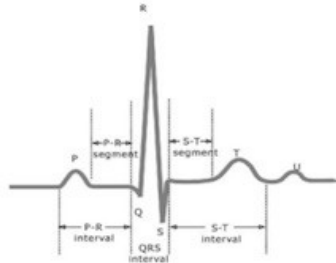


Figure 1.1 ECG waveform [2].

Photoplethysmography: During each cardiac cycle, the blood vessels pulsate in order to carry blood to/from different parts of the human body. When light radiation such as infrared is passed through a blood vessel in a finger or ear lobe, the received light signal from finger/earlobe are periodic and vary due to the rhythmic flow and absorption properties of blood. This optical variation is employed to make Photoplethysmographs. Photoplethysmography is of two types of transmission and reflection based on the place from which the light sensed. In this implementation, an IR LED is excited by a modulated signal to avoid low frequency interference and the received light from finger or ear lobe is sensed by a photodiode which is filtered using a band pass filter with synchronous demodulator which is in sync with the modulator. This is digitized by an ADC and passed through software filters to shape the pulse. The heart rate is determined using a software peak detector [2].

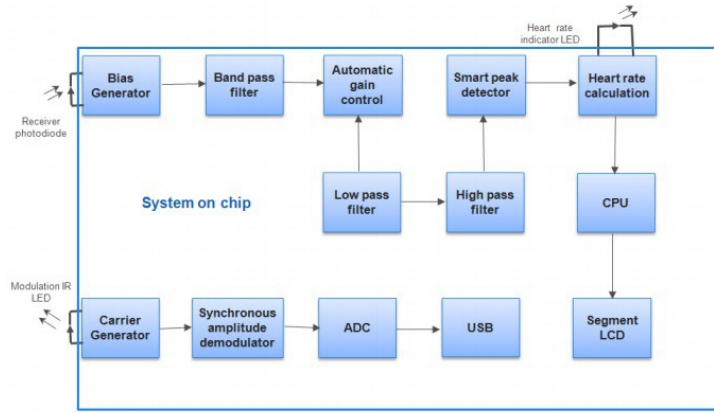


Figure 1.2 Photoplethysmographs [2].

Phonocardiograph: The opening and closing of valves in the heart produces sounds during contraction and dilation which is normally audible through a stethoscope. These sounds are rhythmic to heart beat and can be sensed using microphones. Normal heart sounds are used to determine the heart rate. The normal heart sounds and different murmurs have different spectral characteristics so with proper filtering the abnormalities of the heart can be visualized. This acoustic property is used in phonocardiographs to determine the heart rate [2].

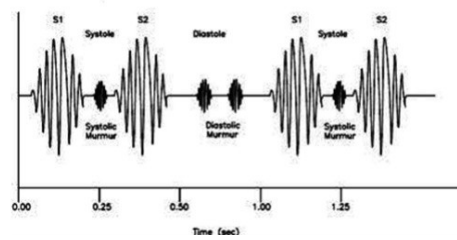


Figure 1.3 Heart Sounds [2].

1.2 GOAL and APPROACH

The goal of this thesis is to analyze and design a multi-port quasi-passive receiver. The design will be performed in Advanced Design System (ADS). This work will

include the implementation in ADS of a heterodyne radio receiver on system level, i.e., based on behavioral models of the included circuits. Then, the multi-port receiver will be designed and simulated. Finally, the possibility of the application of the multi-port receiver for radar applications will be analyzed. A monostatic radar with direct conversion multi-port technology will be considered for the heartbeat and breathing detection.

Project Specifications

- The heterodyne receiver will be implemented for a 60 GHz, quadrature demodulation scheme with ADS behavioral models.
- Knowledge about Circuit Envelope simulation together with generation of complex modulated signals in ADS will be acquired.
- The multi-port correlator will be based on the design of 90° hybrid couplers and Wilkinson power divider, at 2.5 GHz.
- The design will include also generation of the component's layout.
- The microwave sensor will be analyzed mathematically and simulations will be performed.

The entire multi-port receiver will be implemented with real-life components.

1.3 OUTLINE of the THESIS

This thesis consists of 5 chapters, all of them are discussed independently. The following chapters are included:

Chapter 1: Introduction - First chapter is a brief introduction to this project. It gives an overview on the report and project work.

Chapter 2: Theoretical Background - Second chapter is dealing with the theoretical background belonging to this thesis. It shortly presents the traditional receiver architectures and introduces the Multi-Port receiver. The behavior of the Multi-Port correlator is analyzed using a mathematical model.

Chapter 3: Modelling in of a Heterodyne Receiver – It presents a reference modelling of a heterodyne receiver in Advanced Design System (ADS) software from Keysight Technologies. It also presents simulation setups that are typical used with complex modulated signals at high frequency.

Chapter 4: Passive Components – It introduces the basic theory of the microwave passive components, i.e., the quadrature branch line coupler and Wilkinson power divider.

Chapter 5: Multi-Port Receiver Design – Fifth chapter presents the design of the Multi-Port correlator and of the Multi-Port receiver, that is modeled and simulated in ADS using real-world components.

Chapter 6: Multi-Port Microwave Sensor – In the sixth chapter, the use of the Multi-Port receiver as a microwave sensor is analyzed.

Chapter 7: Conclusions - Seventh chapter summarizes and concludes the entire report and project work

2. THEORETICAL BACKGROUND

In this Chapter the basic theory related to this project is presented. The focus will be on the traditional receiver architectures followed by the introduction to Multi-Portreceiver.

2.1 INTRODUCTION

Configurable radio terminals require receivers able to support as many services as possible at different operation frequencies. Classical well-known receivers architectures are limited in this aspect, being designed for specified modulation and demodulation schemes and following certain communication standards. However, other architectures have been introduced, such as six-port receiver. The six-port technique was firstly introduced in the 1960s and 1970s as a flexible and elegant way to perform microwave measurements.

Conventional heterodyne receivers require filters at the RF and IF, which can usually only be implemented by bulky surface acoustic wave or crystal filters. Hence, an integration on a single chip and, thus, small size and low cost, cannot be achieved. For that reason, designers have been directing their effort toward the homodyne receiver, better known as the direct conversion receiver. The direct conversion receiver has gathered much attention, particularly within the research community since then. There are many problems due to analog impairments to be solved when implementing a direct conversion receiver. Therefore, other receiver architectures are sought after. One promising architecture is the multi-port. Moreover, there is always a certain mystery about it. Some publications name it as a “Black box with two inputs and four outputs”. The output ports are terminated with power detectors [7]

Among the first publications on the application of the multi-port communications receivers was Li et al. proved the concept of calculating the complex ratio of an incoming signal and a known local oscillator (LO) signal by using the six-port. Originally, the Multi-Portwas found to be a very good means to measure the complex

reflection coefficient of a microwave device [7]. The initial idea of using a multi-port structure to determinate the phase of a microwave signal was first presented in 1964 by Cohn and Weinhouse [8].

Multi-port configurations are made with the interconnection of several passive circuits, mainly couplers and power dividers. Some examples of multi-port networks are shown in Figure 2.1 [9]. The higher the frequency, the smaller the passive circuit and the easier the integration in a *Monolithic Microwave Integrated Circuit* design.

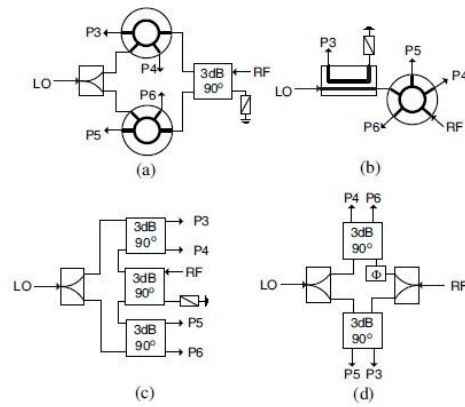


Figure 2.1 Examples of Multi-Port network topologies.

2.2 RECEIVER ARCHITECTURES

The RF front end is a term for all the circuitry between the antenna up to and including the mixer stage. It consists of all the components in the receiver that process the signal at the original incoming radio frequency (RF), before it is converted to a lower intermediate frequency (IF) or to the dc (baseband). This downconversion of the RF signal can be realized in one or several steps [11]. Depending on this, two types of receivers architectures can be distinguished, I.e, the homodyne receiver and the heterodyne receiver. In the homodyne receiver, the carrier frequency is equal to the frequency of the LO signal at the input of the mixer. If the RF and LO1 frequencies are different, the receiver is called the heterodyne.

Today, due to multitude of wireless communication standards, achieving a multi-mode and multistandard receiver is highly desirable. Such receiver must satisfy the

requirements to have broadband or multi-band RF stages, to have low cost, size, and power consumption, and to be compatible with the digital signal processing section. In order to obtain these properties, the RF stage architecture must be chosen properly.

The most usual receiver architectures are presented in Figure 2.2 and 2.3. In Figure 2.2, a direct conversion receiver is shown in form of a block diagram. In this receiver, the RF signal is received by the antenna, filtered and amplified by the low-noise amplifier (LNA). After amplification, the RF signal is downconverted directly to the zero frequency (baseband) as the LO frequency is equal with the carrier frequency of the input RF signal. The main advantage of this receiver architecture is its simplicity and to this contributes also the absence of the image rejection filter, as $\omega_{IF} = \omega_0 - \omega_{LO} = 0$. The main disadvantage is the presence of dc-offsets that might affect correct functionality of the next stages.

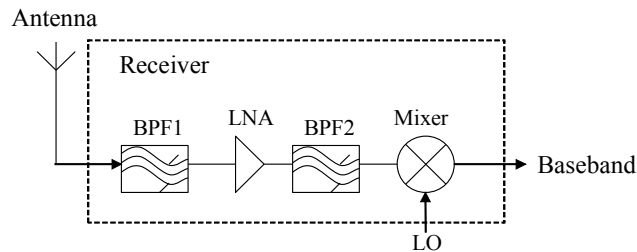


Figure 2.2 Direct conversion (homodyne) receiver architecture.

Heterodyne receiver is the most widely used reception technique and finds numerous applications from personal communication devices to radio and TV tuners. It has been extensively used and is well understood. It comes in a variety of combinations but essentially relies on the same principle. The RF signal is first amplified in a frequency selective low noise stage, then translated to a lower intermediate frequency (IF) with significant amplification and additional filtering, and finally down-converted to baseband with either a phase discriminator or straight mixer, depending on the modulation format. This technique is illustrated in Figure 2.3.

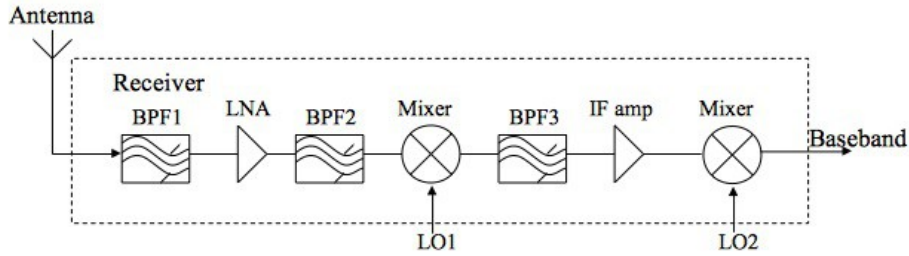


Figure 2.3 Heterodyne receiver architecture.

For most heterodyne architectures Figure 2.3, the RF front end consists of:

An *impedance matching* circuit to match the input impedance of the receiver with the antenna, so the maximum power is transferred from the antenna.

A *band-pass filter* (BPF) to reduce strong out-of-band signals and image frequency response.

An *RF amplifier*, often a *low-noise amplifier* (LNA). Its primary responsibility is to increase the sensitivity of the receiver by amplifying weak signals without contaminating them with noise, so that they can stay above the noise level in succeeding stages. It must have a very *low-noise figure* (NF). The RF amplifier may not be needed and is often omitted (or switched off) for frequencies below 30 MHz, where the signal-to-noise ratio is defined by atmospheric and man-made noise.

A first *local oscillator* (LO1) which generates a signal at a frequency offset from the carrier signal. By mixing operation, the RF signal is downconverted to an *intermediate frequency* (IF), ω_{IF} .

The second mixer in Figure 2.3 downconverts the IF signal to zero frequency by choosing $\omega_{\text{LO2}} = \omega_{\text{IF}}$.

2.3 FREQUENCY-CONVERSION

Frequency conversion is the process of shifting the spectrum of a signal. There are several reasons for doing this, i.e., the separation of a certain number of signals on a transmission medium (using different carrier frequencies) or to be able to radiate a signal by an antenna. The signal $X_{bp}(f)$ is shifted by f_0 resulting in $X_{bp}(f-f_0)$. We can conclude that the frequency shift can be achieved by multiplying the signal $X_{bp}(f)$ with

the exponential function. This function must be reduced into $\cos(2\pi f_0 t)$ and $\sin(2\pi f_0 t)$. Then, we can expand the $\cos(2\pi f_0 t)$ to $1/2(e^{j2\pi f_0 t} + e^{-j2\pi f_0 t})$ reveals that the real frequency conversion results in two separate frequency shifts of the original spectrum $X_{bp}(f)$. (Figure 2.1 [14]).

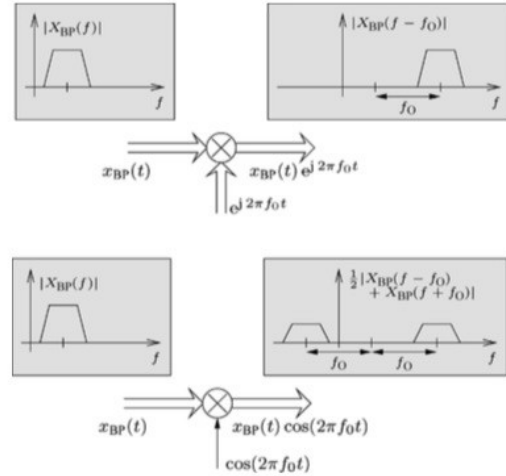


Figure 2.4 Real frequency conversion.

2.4 The MULTI-PORT RECEIVER

The multi-port receiver consists of the Multi-Port correlator and a few components, diodes or transistors, used to perform power detection and thus to complete the process of down-conversion from carrier frequency to either IF-frequency or baseband frequency. It was firstly used for microwave measurements. First work for microwave measurements with the multi-port correlator has been conducted by G. F. Engen and C. A. Hoer [4,5].

The multi-port correlator is shown in Figure 2.5. It consists of one Wilkinson power divider (WPD) and three quadrature branch line couplers (QBLC), [15]. These are passive structures using the properties of quarter-wave transmission ($\lambda/4$) lines to delay the incoming signals with an accurate phase difference, i.e., 90° . In addition, when two input signals are used, as shown in Figure 2.5, superposition of these signals takes place, so that at the output ports, P3 - P6, the signals can be written as:

$$P3: \frac{S_{RF}(t)(-j)^2}{2} + \frac{S_{LO}(t)(-j)^4}{2} = \frac{-S_{RF}}{2} + \frac{S_{LO}}{2} \quad (1)$$

$$P4: \frac{S_{RF}(t)(-j)^3}{2} + \frac{S_{LO}(t)(-j)^3}{2} = \frac{j S_{RF}}{2} + \frac{\mathcal{S}_{LO}}{2} \quad (2)$$

$$P5: \frac{S_{RF}(t)(-j)^2}{2} + \frac{S_{LO}(t)(-j)^3}{2} = \frac{-S_{RF}}{2} + \frac{\mathcal{S}_{LO}}{2} \quad (3)$$

$$P6: \frac{S_{RF}(t)(-j)^3}{2} + \frac{S_{LO}(t)(-j)^2}{2} = \frac{j S_{RF}}{2} + \frac{-S_{LO}}{2} \quad (4)$$

The superposition of the LO and RF signals at ports P3 to P6 can be written in time-domain as:

$$P3: -A_{RF} \cos \alpha + A_{LO} \cos (\beta + \pi/2) = -A_{RF} \cos \alpha - A_{LO} \sin (\beta) \quad (5)$$

$$P4: A_{RF} \cos (\alpha + \pi/2) - A_{LO} \cos (\beta) = -A_{RF} \sin \alpha - A_{LO} \cos (\beta) \quad (6)$$

$$P5: A_{RF} \cos (\alpha) + A_{LO} \cos (\beta) \quad (7)$$

$$P6: A_{RF} \cos (\alpha + \pi/2) - A_{LO} \cos (\beta + \pi/2) = -A_{RF} \sin \alpha - A_{LO} \sin (\beta) \quad (8)$$

Where $\alpha = \omega_{LO} t + \theta(t)$ and $\beta = \omega_{LO} t$.

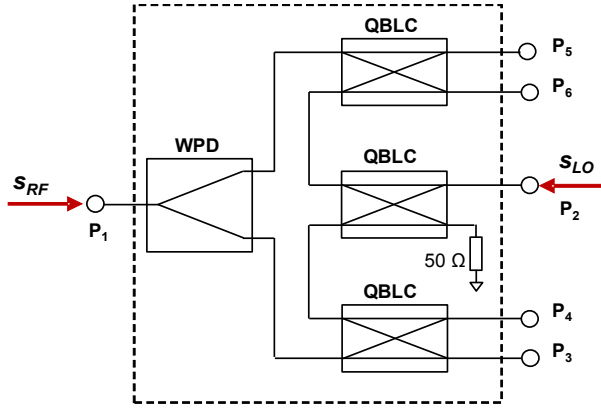


Figure 2.5 Multi-Port correlator with assigned input signals s_{RF} and s_{LO} [16].

The multi-port correlator can be used together with power detection diodes in order to implement a Multi-Port receiver. The multi-port receiver shown in Figure 2.6 allows separation of I and Q base-band channels working as a quadrature demodulator. With reference to Figure 2.5, the modulated radio frequency (RF) signal applied to P_1 and containing the I and Q data is linearly combined with LO signal applied at P_2 . The output signals O_3-O_5 and described by (5) to (8) in Figure 2.6 are processed by the diodes with squaring operation, $(\bullet)^2$, generating after LP filtering the down-converted signals W_3-W_5 .

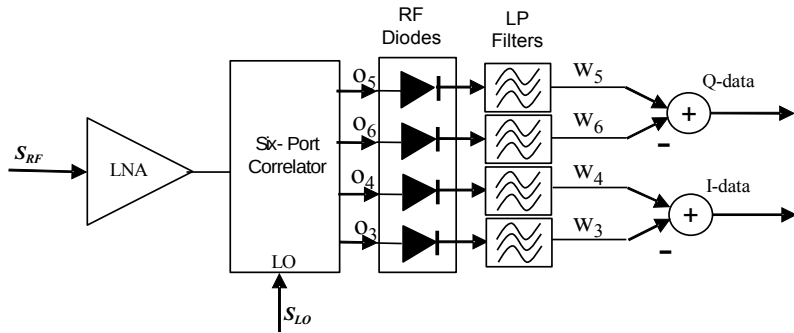


Figure 2.6 Direct conversion Multi-Port receiver using diodes as power detectors [17].

The corresponding equations modelling above described process of down-conversion are presented as follows.

$$S_{RF}(t) = R(t) \cos(\omega_{LO}t + \theta(t)) \quad (9)$$

$$S_{LO}(t) = A_{LO} \cos(\omega_{LO}t) \quad (10)$$

$$W_3(t) = -A_{BB,I} \cos(\theta(t)) \quad (11)$$

$$W_4(t) = A_{BB,I} \cos(\theta(t)) \quad (12)$$

$$W_5(t) = -A_{BB,Q} \sin(\theta(t)) \quad (13)$$

$$W_6(t) = A_{BB,Q} \sin(\theta(t)) \quad (14)$$

W_3 - W_5 equations demonstrate that the multi-port correlator together with the nonlinear processing of the power detectors allow to separate the I and Q baseband channels. In reality, the demodulated signals W_3 - W_5 will not only contain the desired baseband information but also a dc offset terms.

In a multiport heterodyne receiver, the carrier frequency ω is similar in value to the local oscillator frequency ω_0 . Hence, if $\omega_0 = \omega$, I/Q direct conversion is obtained in a homodyne architecture. This fact can be considered as an important advantage of the proposed receiver compared to the conventional down-conversion receiver. The same multiport front-end can be used for both heterodyne and homodyne architectures.

Moreover, signal to noise ratio is improved using a multiport circuit. In addition, it used two Shottky diodes is compensated by the reduced cost of the IF stage. When digital modulation schemes are involved, quadrature mixers are employed to both modulate the carrier and demodulate the digitally modulated RF signal. In this case, the baseband signal is processed and mapped into in-phase (I) and quadrature phase (Q) signals, where it is worth to mention att I- and Q- are still baseband signals [13].

3. HETERODYNE RECEIVER MODELLING

The use of simulation to design electrical systems and components is not only of practical meaning, but also necessary as the complexity of communication systems constantly increases. Designing and optimizing these systems and components often requires a good understanding of the systems and of the parameters and variables that influence the system performance. Simulation lets the designer take these variables into account in a only one environment and helps reduce the time for system design.

In this project, the Advance Design System from Keysight Technologies will be used. In this chapter, a heterodyne receiver will be implemented and simulated as a reference design for complex receivers. This receiver will make use of circuits described on behavioral level and no real-world circuits will be designed or used. Focus will be on simulation set-ups for this kind of receivers. Then, in the next chapters, a homodyne multi-port receiver will be implemented. In this second case, the main circuits of the receiver will be designed using real-world components described by vendor's models.

The ADS implementation of the heterodyne receiver is shown in Figure 3.1. The received signal is an RF QPSK modulated signal. Simulations are performed using a 60 GHz carrier frequency and the IF of the heterodyne receiver was chosen at 900 MHz.

The second frequency conversion using behavioral mixers regenerated the I-and-Q-baseband signals.

The RF stage contains the amplifier (AMP1), mixers 1-2 and BPF Butterworth filter and I/Q mixer. It can be seen the typical architecture of a IF and baseband stage: IF down-converters (MIX1, MIX2, LPF1, AND LPF2) and a couple of sample-and-hold circuits (SAMP1 and SAMP2).

The general overview of the heterodyne receiver simulation block diagram, using ADS software, can be seen in Figure 3.1.

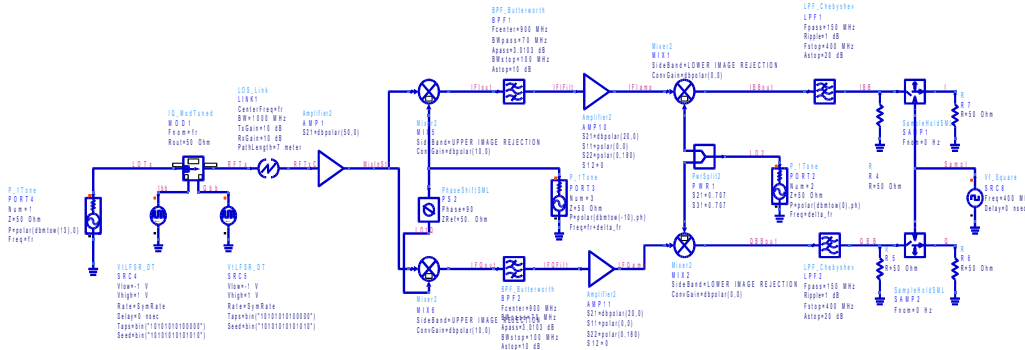


Figure 3.1 ADS multiport heterodyne receiver.

It can be seen the characteristics heterodyne receiver in Figure 3.2. It had been used two mixers (Sideband UPPER IMAGE REJECTION), two Butterworth filters and two amplifiers.

Each of them have some characteristics that are summarized below:

Mixer (Sideband UPPER IMAGE REJECTION): It produces symmetric image rejection at the upper and lower image band edges.

BFP Butterworth is one of the most basic filter. It is used in order to obtain the flattest possible response to the cutoff frequency.

The frequency response of the filter is extremely flat (with minimum ripples) in the passband.

In comparison with the Chebyshev filters (They are used in the demodulation stage), they have a different response at low frequencies because they allow ripples in one of his bands.

Most *Amplifiers* work reasonably well at lower frequencies, but at high frequencies often the device S.S. Model is not accurate enough. So, using s-parameters can be a good way to obtain an accurate amplifier. The s-parameter design uses relationships between input and output powers, forward and reflected powers. They are used to improve the overall gain of the receiver.

3.1 TRANSMITTER BLOCK DIAGRAM

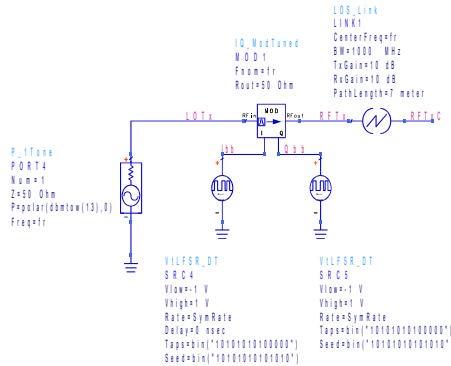
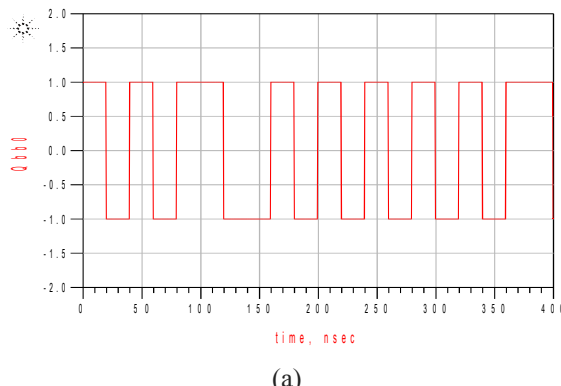
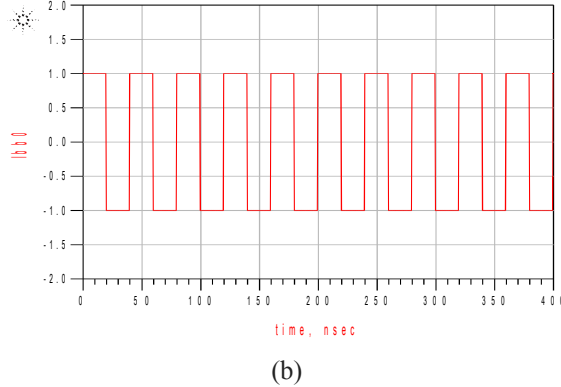


Figure 3.2 ADS transmitter block diagram.

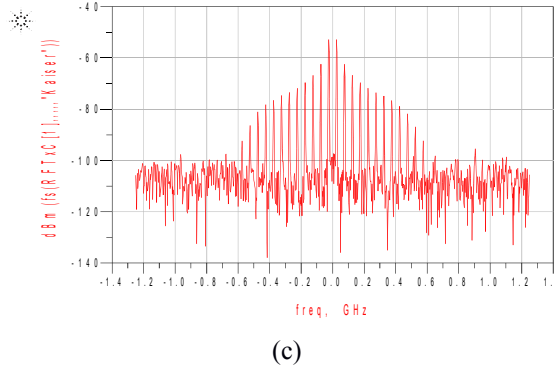
Simulations are performed using a 60 GHz carrier frequency, the IF of the heterodyne receiver was chosen at DELTA_FR (900 MHz) in order to obtain a QPSK signal. It is used a 100 Mbps QPSK signal generated at the signal transmitter with two baseband data generators connected to the I/Q modulator block (see Figure 3.1).



(a)



(b)



(c)

Figure 3.3 Simulated Results. (a) Ibb signal in ADS, (b) Qbb signal in ADS and (c) RFTxC signal in ADS.

3.2 RF to IF – PROCESSING BLOCK

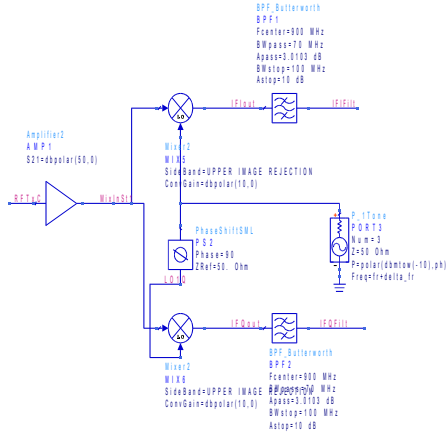
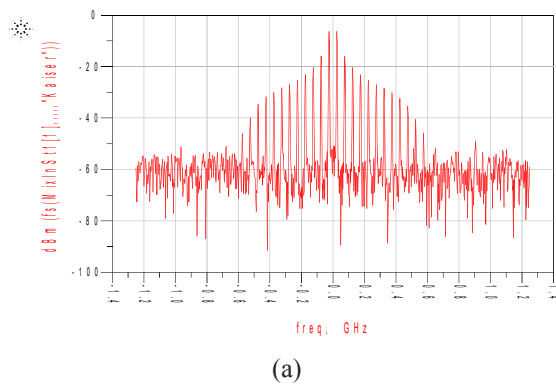


Figure 3.4 ADS processing block.

The RF stage contains the amplifier (AMP1), mixers 1-2 and BPF Butterworth filter and I/Q mixer (Figure 3.4). It can be seen the typical architecture of a IF and baseband stage (Figure 3.5).



(a)

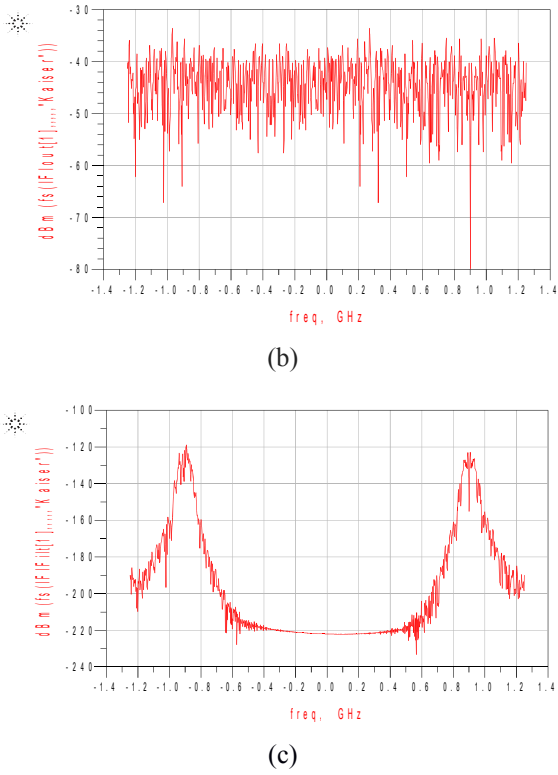


Figure 3.5 Simulated Results. (a) MixInSt1 signal in ADS, (b) IFlout signal in ADS and (c) IFIFilt signal in ADS.

3.3 IF to BASEBAND PROCESSING BLOCK

Simulation results are shown in Figure 3.7. The I/Q components are amplified and the signals go through the MIXER2 obtaining the two baseband signals IBBout and QBBout. Coming up next, they are filtered.

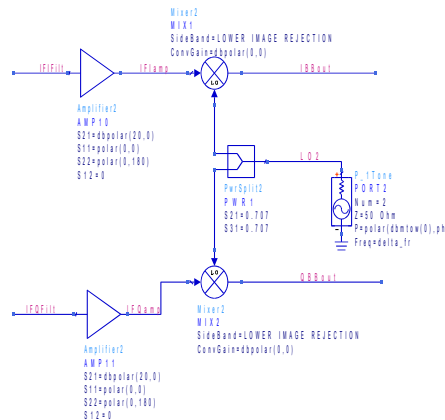
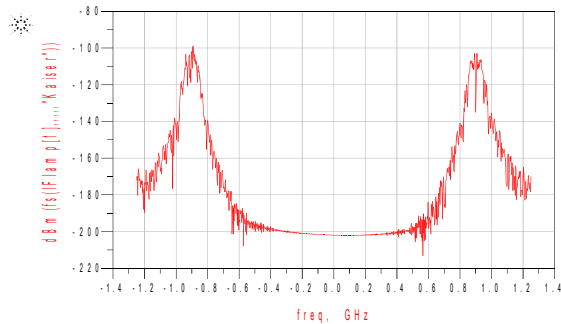
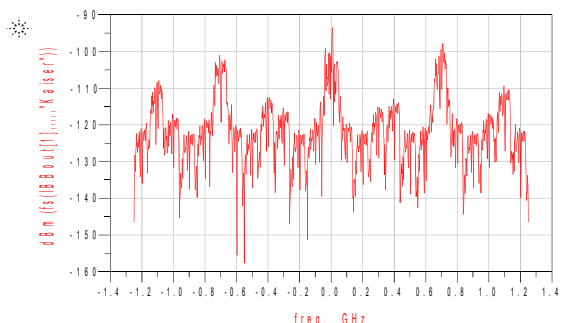


Figure 3.6 IF-BB converter diagram block.



(a)



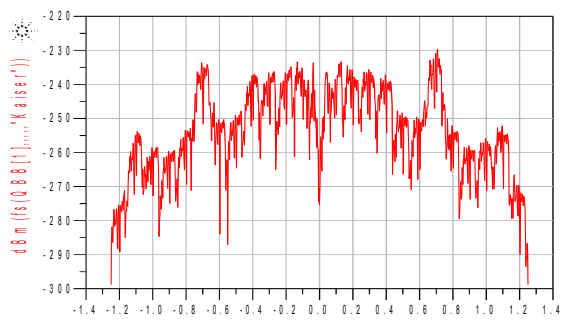
(b)

Figure 3.7 Simulated Results. (a) IFIamp signal in ADS and (b) IBBout signal in ADS.

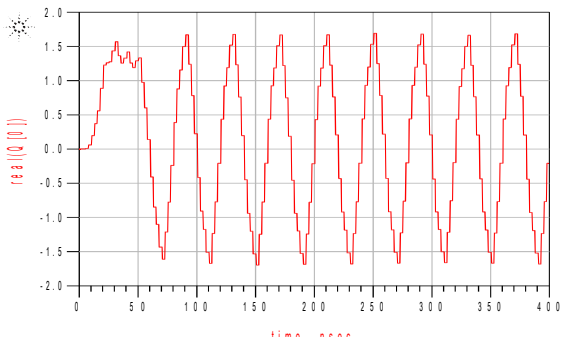
Signal before/after the mixer.

3.4 SAMPLING I/Q SIGNALS

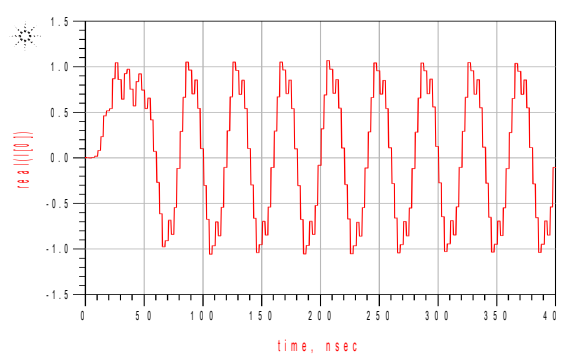
In this step the analog to digital conversion of the baseband signals are taken. We obtained the same digital I/Q signals and I/Q transmitted data (see Figure 3.8).



(a)



(b)



(c)

Figure 3.8 Simulation Results. (a) QBB signal in ADS, (b) Q signal in ADS and (c) I signal in ADS.

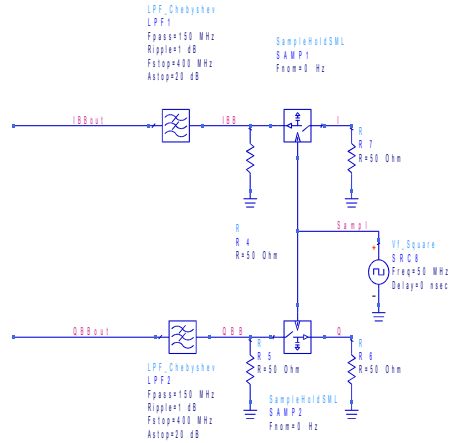


Figure 3.9 Sampling of the final signal.

4. PASSIVE COMPONENTS

In this chapter it is introduced the basic theory of the microwave passive components, i.e., the quadrature branch line coupler and Wilkinson power divider. Also, the design of these components is presented.

BRANCH COUPLER

Directional couplers can be made in many different forms, they are four-port circuits where one port is isolated from the input port. All ports are matched, and the circuit is lossless. Most of the times, they are used for sampling a signal. They usually use distributed properties of microwave circuits, for example, the coupling feature is generally quarter-wavelengths. One of the ports is called “coupled”, another one is called “isolated” which is normally terminated, the third one is called “through” (where the signal incident exists) and the last one is called “input”. The coupled port is a function of which port is the incident port.

It is shown in Figure 4.1 [18]:

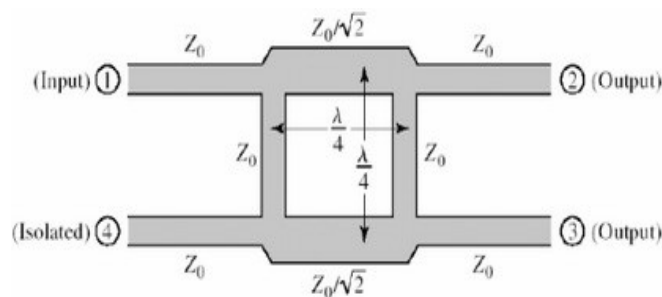


Figure 4.1 Geometry of a branch-line coupler.

THE QUADRATURE (90° HYBRID):

The 90° Hybrid Coupler is a 4-port device, It is known as the quadrature coupler or branch-line coupler. Its scattering matrix has the symmetric solution for a matched, lossless, reciprocal 4-port device. They have a 90° phase difference between “through”

and “coupled” outputs. It is used in microstrip and stripline. Other 3 dB couplers can also work as a quadrature coupler.

It works as follows, power goes through port 1 and it is divided in ports 2 and 3, with a 90° phase shift between these outputs. No power goes through port 4 (isolated port).

Observe that the branch-line hybrid has a high degree of symmetry, as any port can be used as the input port. Any port can be used as a input port. The output ports will always be on the opposite side of the junction from the input port, and the isolated port will be the remaining port on the same side as the input port. This symmetry is reflected in the scattering matrix, as each row can be obtained as a transposition of the first row.

Thus, the [S] matrix will have the following form [18]:

$$[S] = \begin{bmatrix} S_{11} & S_{12} & S_{13} & S_{14} \\ S_{21} & S_{22} & S_{23} & S_{24} \\ S_{31} & S_{32} & S_{33} & S_{34} \\ S_{41} & S_{42} & S_{43} & S_{44} \end{bmatrix} = \frac{-1}{\sqrt{2}} \begin{bmatrix} 0 & j & 1 & 0 \\ j & 0 & 0 & 1 \\ 1 & 0 & 0 & j \\ 0 & 1 & j & 0 \end{bmatrix}$$

EVEN - ODD MODE ANALYSIS:

We first work with the schematic circuit of a branch-line coupler in normalized form, as in in Figure 4.2. Each line represents a transmission line with indicated characteristic impedance normalized to Z_0 . The common ground return for each transmission line is not shown. We assume that a wave of unit amplitude $A_1 = 1$ is incident at port 1.

The circuit can be descomposed into the superposition of an even-mode excitation and odd-mode excitation (Figure 4.2 [18]). The superimposing of the two sets of excitations produces the original excitation and since the circuit is linear, the actual response can be obtained from the sum of the responses to the even and odd excitations.

Due to the symmetry or antisymmetry of the excitation, the four-port network can be decomposed into a set of two decoupled two-port networks.

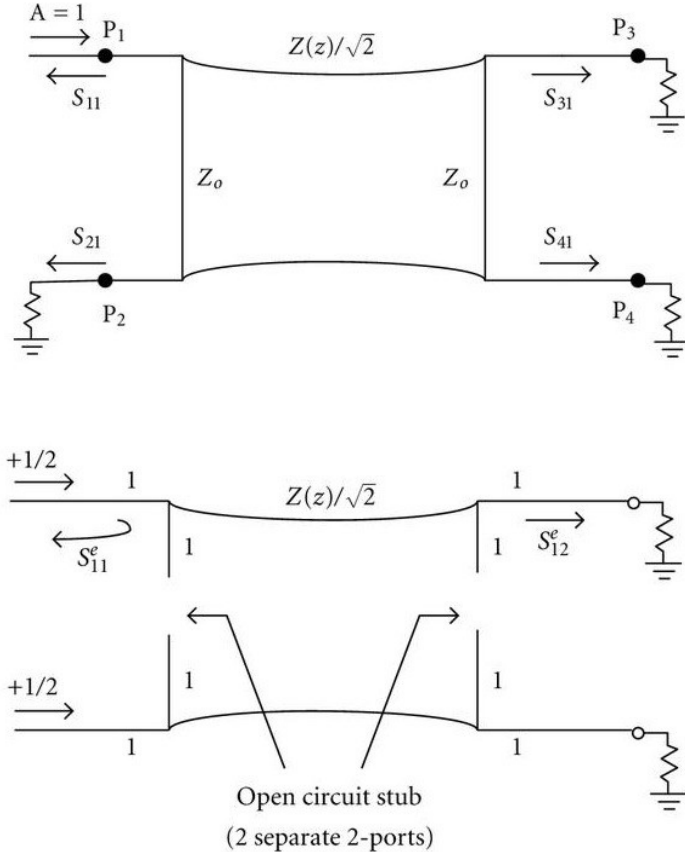


Figure 4.2 Descomposition of the branch-line coupler into even-odd mode excitations.

Since the amplitudes of the incident waves for these two-ports are $+/- \frac{1}{2}$, the amplitudes of the emerging wave at each port of the branch-line hybrid can be expressed as [18]:

$$B_1 = \frac{1}{2} \rho_e + \frac{1}{2} \rho_o, \quad (1)$$

$$B_2 = \frac{1}{2} T_e + \frac{1}{2} T_o, \quad (2)$$

$$B_3 = \frac{1}{2} T_e - \frac{1}{2} T_o, \quad (3)$$

$$B_4 = \frac{1}{2} \rho_e - \frac{1}{2} \rho_o, \quad (4)$$

Where ρ_e , ρ_o and T_e , T_o are the even-and odd-mode reflection and transmission coefficients for the two-port networks.

First consider the calculation of ρ_e and T_e , for the even-mode two-port circuit.

$$P_e = \frac{A+B-C-D}{A+B-C-D} = \frac{(-1+j-j+1)/\sqrt{2}}{(-1+j+j+1)/\sqrt{2}} = 0 \quad (5)$$

$$T_e = \frac{2}{A+B-C-D} = \frac{2}{(-1+j+j-1)/\sqrt{2}} = \frac{-1}{\sqrt{2}} (1+j) \quad (6)$$

Which gives the reflection and transmission coefficients as [9]:

$$\rho_0 = 0 \quad (7)$$

$$T_0 = \frac{1}{\sqrt{2}} (1-j) \quad (8)$$

Then, we obtain the following results [9]:

$$B_1 = 0 \quad (\text{port 1 is matched}), \quad (9)$$

$$B_2 = \frac{-j}{\sqrt{2}} \quad (\text{half-power, } -90^\circ \text{ phase shift from 1 to 2}), \quad (10)$$

$$B_3 = \quad (\text{half-power, } -180^\circ \text{ phase shift from 1 to 3}), \quad (11)$$

$$B_4 = 0 \quad (\text{no power to port 4}), \quad (12)$$

The results match with the [S] matrix. The bandwidth of a branch-line hybrid can be increased to a decade or more by using multiple sections in cascade.

4.1 SCHEMATIC LEVEL DESIGN in ADS

Firstly, the PCB substrate is defined. his substrate (FR4) will be used through the entire thesis.

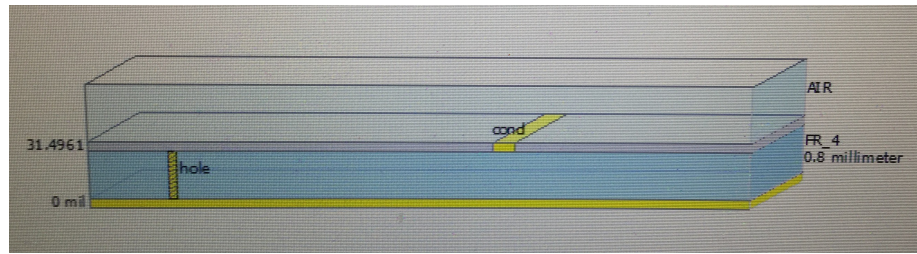


Figure 4.3 FR4 substrate representation in ADS.

In order to characterize the FR4 substrate it has made some adjustments:

The top light part should be AIR.

On the layer “cond”, the material should be Copper with a thickness of 18 micron and without any surface roughness.

On the layer “hole” the material should be PERFECT_CONDUCTOR and none surface roughness.

On the substrate layer “FR_4” it should have a thickness of 0.8 millimeter.

Between Air and substrate layer “FR_4”, the interface should be a strip plane, and the bounding are layer and they should be inherit from the substrate.

The last interface, in yellow colour, should be cover with a thickness of 0 micron.

The circuit will be simulated for both transient behaviour and S-parameters estimation. They will be working for the specified central frequency, in this case, 2.5 GHz. It has been created a variable called f_0 for this value. The frequency response of the circuit will be chosen for +/- 1GHz, using a step size of 10 MHz. The time-domain simulation has a StopTime of 3.5 nsec, and a maximum step-size of 10 nsec.

The substrate FR4 was defined with a TanD of 0.02, it has a relative permittivity (ϵ_r) of 4.6, it has 0 mm of roughness and a relative permeability (μ_r) of 1 (Nonmagnetic material). The remainder of the power from port 3 passes through to the output port (pin 2). At the center frequency (2.5 GHz). There is a phase difference of 90° between the outputs. The coupling coefficient specifies the ratio of the input power to the coupled power. Pin 4 is the isolated port, and it is typically well isolated from the input port near the center frequency.

The substrate FR4 was defined with a TanD of 0.02, it has a relative permittivity (ϵ_r) of 4.6, it has 0 mm of roughness and a relative permeability (μ_r) of 1 (Nonmagnetic material). The remainder of the power from port 3 passes through to the output port (pin 2). At the center frequency (2.5 GHz). There is a phase difference of 90° between the outputs. The coupling coefficient specifies the ratio of the input power to the coupled power. Pin 4 is the isolated port, and it is typically well isolated from the input port near the center frequency.

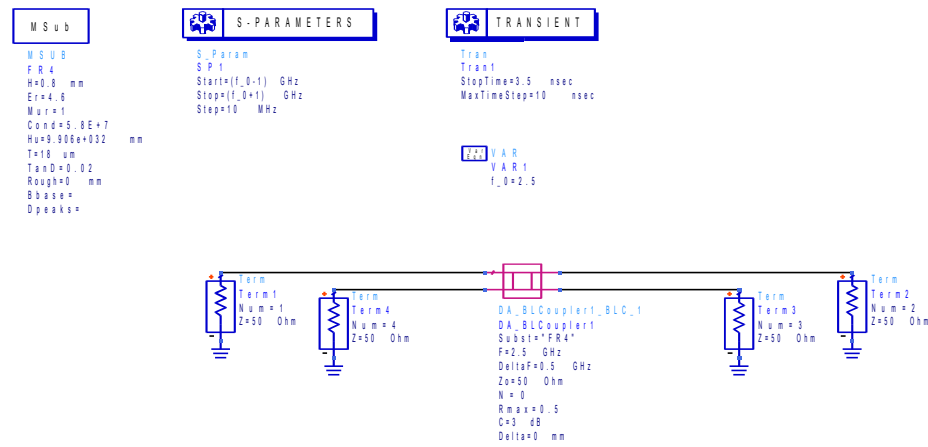


Figure 4.4 Smart component with S-parameter and Transient parameter simulation set-up.

4.2 LAYOUT LEVEL DESIGN in ADS

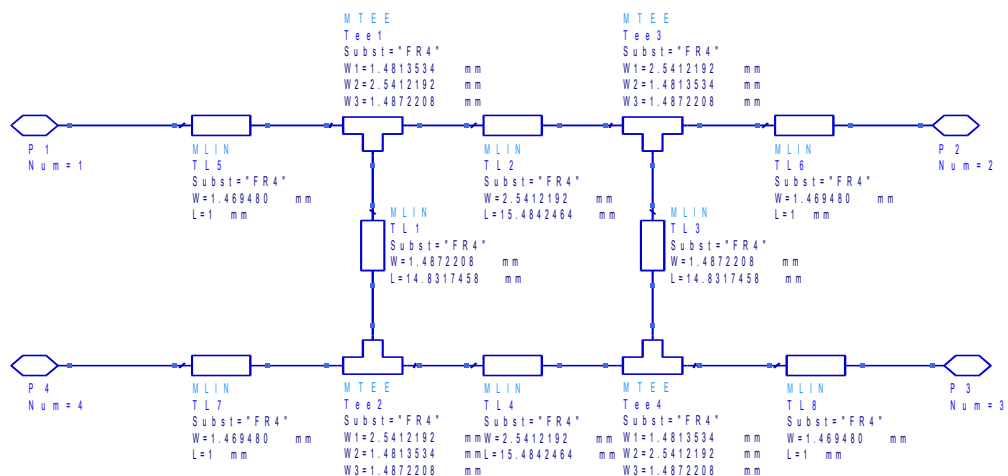


Figure 4.5 Schematic of the microstrip branch line coupler.

Momentum, is a part of ADS that permits to generate S-parameters simulations for general planar circuits, such as stripline, etc... We should select a “Frequency plan” in the ADS. Firstly, we set “Adaptative” type of frequency and it was decided to take 1.5 GHz as a Fstart and 3.5 GHz as Fstop and finally Npts = 40. When the schematic Fig.4.5 was generated, it should be added four identical transmission lines of 50Ω characteristic impedance to the four ports of the BLC.

4.3 S - PARAMETER

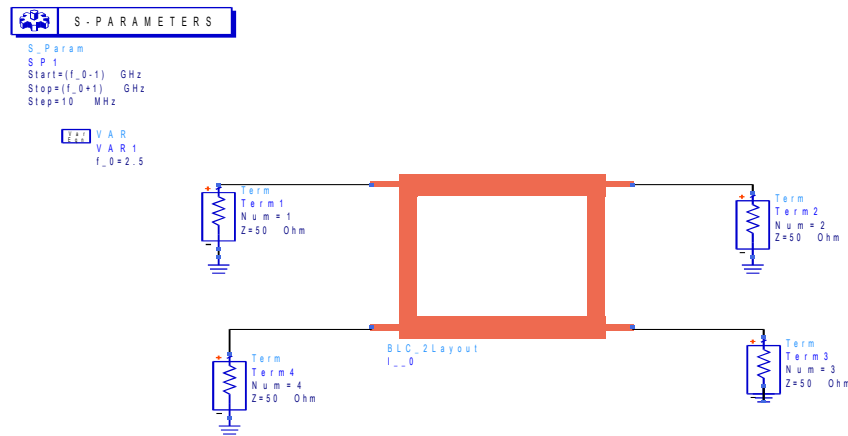
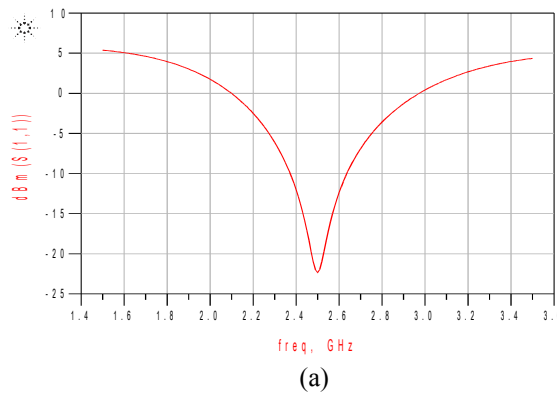


Figure 4.6 The Wilkinson power divider as a layout component S-parameters simulation set-up.

The results were optimized for the frequency given. In this case, 2.5 GHz.



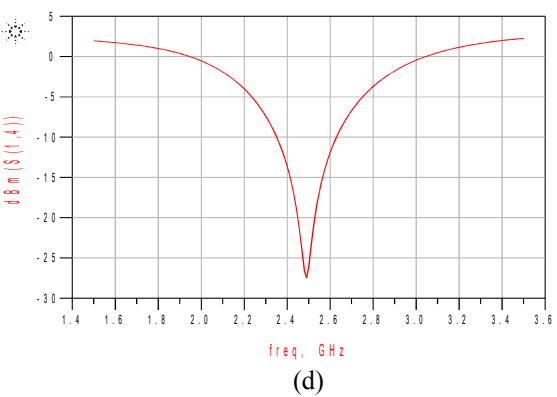
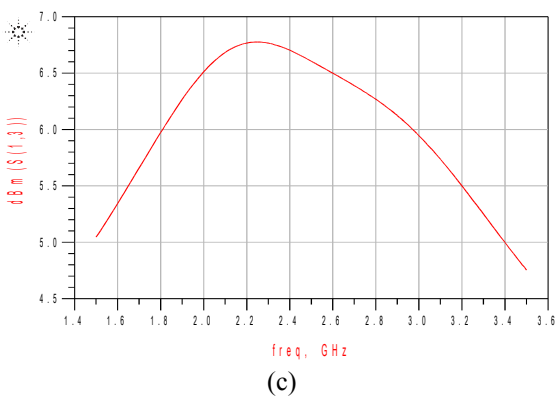
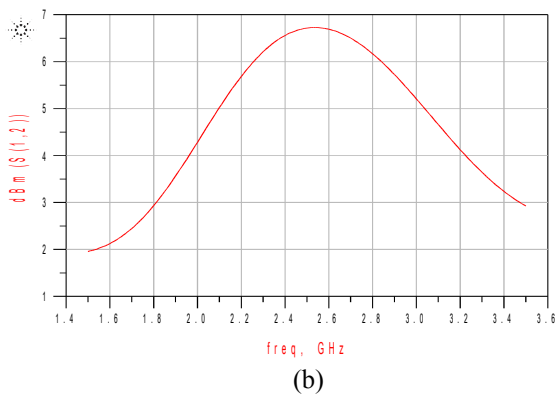


Figure 4.7 Simulated S-parameters of the Branch Coupler (a) S(1,1) parameter, (b) S(1,2) parameter, (c) S(1,3) parameter and (d) S(1,4) parameter.

S-parameters are common used for networks which are operating at radio frequency (RF) and microwaves frequencies where signal power and energy considerations are

more easily quantified than currents and voltages. They are conceptually simple, analytically convenient, and capable of providing a great insight into a measurement or design problem. The coupling coefficient must be positive and greater than 3 dB.

The above figure implies that the branch coupler works best at 2.5 GHz, where $S(1,1) = -22$ dB. Further, at 2.1 GHz it will radiate virtually nothing, as $S(1,1)$ is close to 0 dB (so all the power is reflected). The branch-line bandwidth can also be determined from the above figure. If the bandwidth is defined as the frequency range where $S(1,1)$ is to be less than -5 dB, then the bandwidth would be roughly 0.5 GHz, with 2.3 GHz the high end and 2.8 GHz the low end of the frequency band.

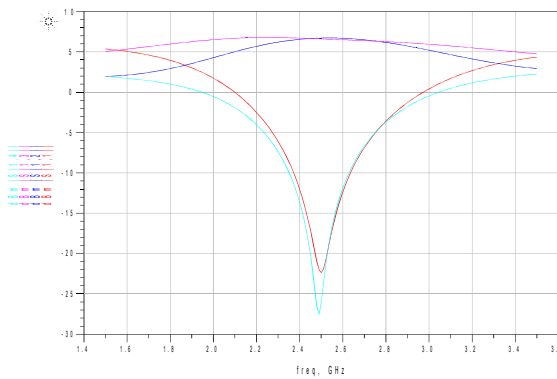


Figure 4.8 Simulated S-parameters. $S(1,1)$, $S(1,2)$, $S(1,3)$, $S(1,4)$.

The optimization minimizes the input reflection coefficient $S(1,1)$ at the design center frequency by changing the length of the lines forming the four branches. All branches are changed by the same physical length during the optimization. Although, it doesn't assure that the branch-line will work at the frequency desired.

As it is shown in Figure 4.8 Parameters $S(2,1)$ and $S(3,1)$ have almost the same reflection coefficient of -3.27 and -3.38 respectively. $S(4,1)$ is an isolated port as it can be inferred from the results (the value is so small), -36.33. Thus, we can see that it is an optimised Branch Coupler Design.

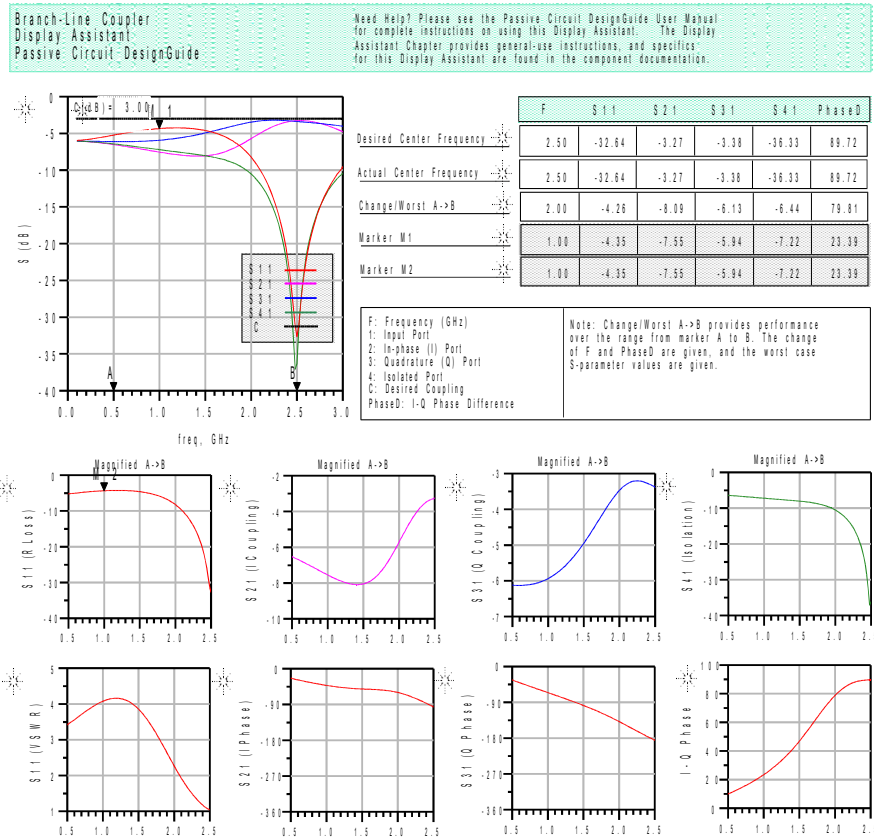


Figure 4.9 Optimized parameters.

4.4 TRANSIENT SIMULATION

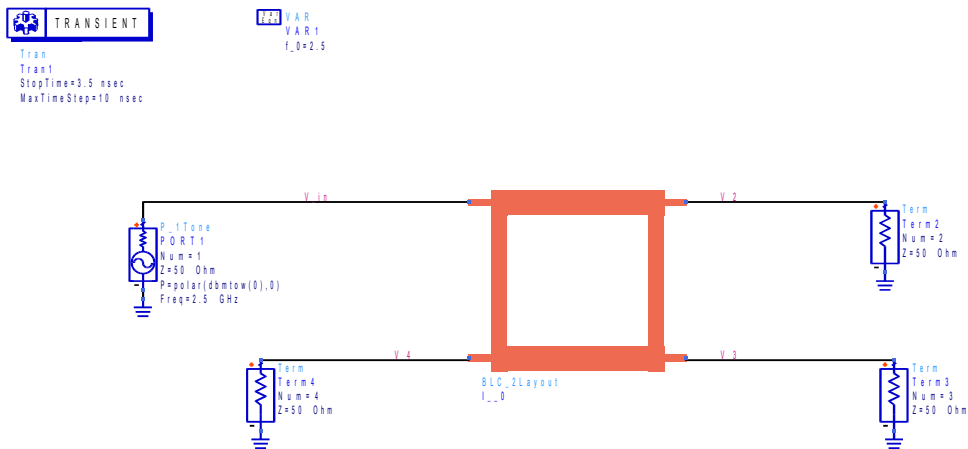
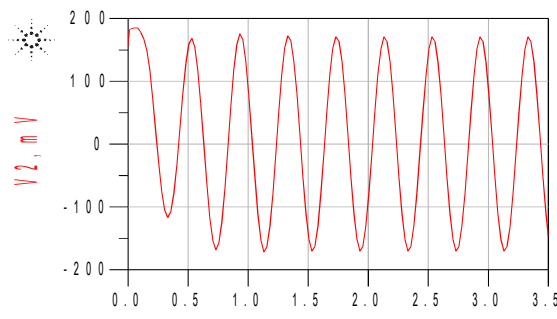
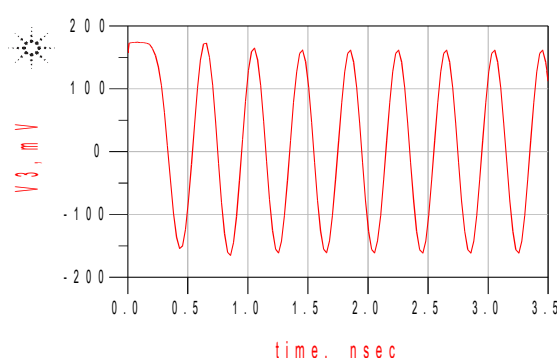


Figure 4.10 The Branch line coupler as a layout component and simulation set-up.

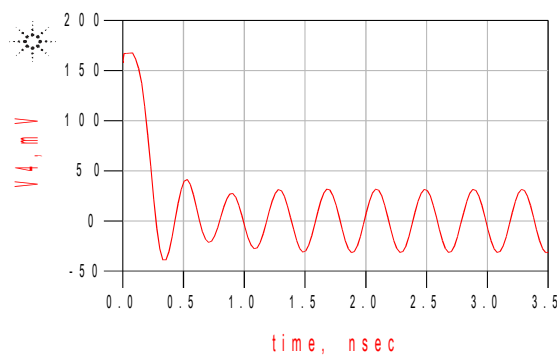
Transient simulations can only be performed when you apply a time-domain signal, for example, sine wave. Thus, you need a P_1Tone source at port1 and labels on the output termination wires to display them after simulation. It was chosen a $Z = 50 \Omega$ and the frequency given 2.5 GHz. All the outputs were labelled clockwise as shown in Fig. 4.10. The results were optimize fo the frequency given. In this case, 2.5 GHz.



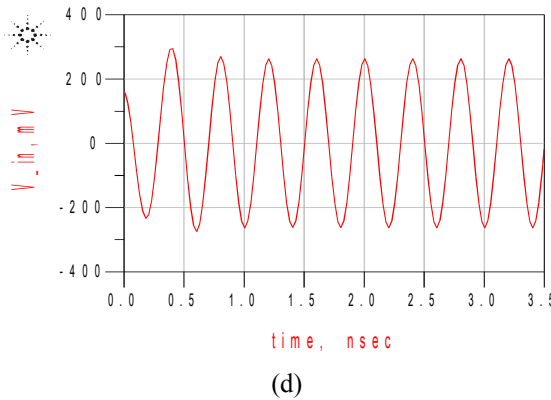
(a)



(b)



(c)



(d)

Figure 4.11 Transient Simulation. (a) V_2 , (b) V_3 , (c) V_4 and (d) V_{in} .

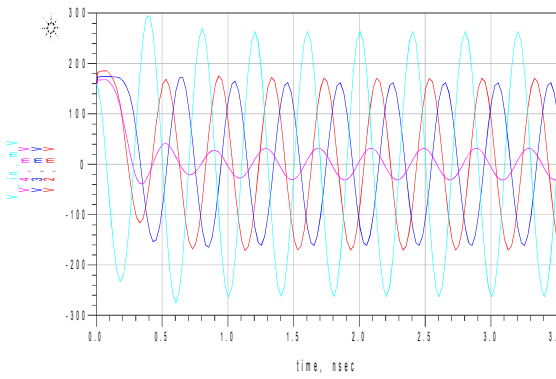


Figure 4.12 Transient Simulation. V_2 V_3 V_4 V_{in} .

Transient analysis always begins at time = 0, and assumes that only the DC sources were connected to the circuit at that time. Transient analysis saves node voltages and branch currents at each time point in the analysis. Smaller time steps in transient analysis improve measurement accuracy.

As it is shown in Figure 4.11 (a) and Figure 4.11 (b), both of them, are similar in amplitude but V_4 shown in Figure 4.11 (c) is totally different. Port4 is totally isolated because it has a big amplitude.

It was taken a Stop_time of 3.5 nsec in order to see 4 signal periods shown in Figure 4.12.

THE WILKINSON POWER DIVIDER

The Wilkinson power divider is a network, with the property of being lossless when the output ports are matched, only reflected power is dissipated, it hasn't got any isolation between output ports.

In this type of dividers, there are four different sections.

Input port

Quarter-wave transformers

Isolation resistors

Output ports

Input and output ports are identical and the value of the impedances of them are Z_0 . Quarter-wave transformer parts are called as quarter-wave transformer because of the length of these parts. The length of these parts are equal to the one fourth of the wavelength of the electromagnetic wave, which is propagating in this three port network.

This length is also related to the operation frequency [19]:

$$\text{Wavelength} * \text{Frequency} = \text{Phase velocity} \text{ (Usually the speed of light)}$$

The reason for this leads us to understand the matching conditions for this network. Matching of the output ports is necessary for the better power transfer from input to output, because if the output ports are matched, the reflected power from the network when we input some amount of power is zero. This means, there is no reflection from the outputs and all of the power is transmitted to the output ports. Consider the case of inputting power at port 1 and terminate the ports 2 and 3 with the reference loads. The scattering parameters for a 2-way Wilkinson power divider reveals that the network is reciprocal ($S_{ij} = S_{ji}$), that the terminals are matched ($S(1,1)$, $S(2,2)$ and $S(3,3) = 0$), the output terminals are isolated ($S(2,3)$, $S(3,2) = 0$). It can not satisfy all three conditions(matched, reciprocal and isolated) at the same time. No loss happens when the signals at ports 2 and 3 are in phase and have equal magnitude. The design of an equal-split (3 dB) Wilkinson is often made in stripline or microstrip form.

One of the biggest drawbacks of the Wilkinson power divider is that it has a quite narrow bandwidth. This can be improved by adding a quarter-wavelength section in front of the power combiner. In this way the impedance transformation is done in two steps, thereby improving the bandwidth. The bandwidth of the power divider can also be increased by splitting the two quarter wavelength sections into multiple sections with a resistor between each section [20]. The Wilkinson power divider can be analyzed in two different circuits by symmetric and antisymmetric sources at the outputs ports (Fig. 4.13).

<u>N</u>	<u>Isolation (dB)</u>
2	∞
3	∞
4	21.6
5	19.5
6	17.6
7	17.2
8	16.1
10	14.9
12	14.1

Fig.4.13 Isolation values for several values of n.

Due to the nature of the Wilkinson power divider under matched conditions, it is obvious that the Wilkinson provides the better power divider performance. Thus, it will be analyzed below [21]:

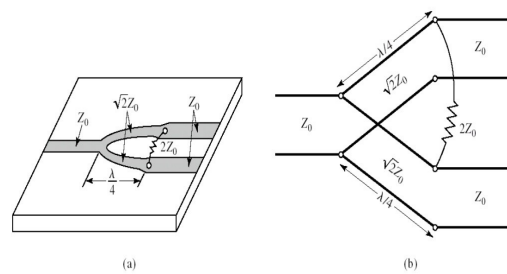


Figure 4.14 (a) An equal-split Wilkinson power divider in microstrip form. (b) Equivalent transmission line circuit.

Even-Odd Analysis:

Even-odd mode analysis uses two important principles:

- a) Superposition

b) Circuit Symmetry

We define two separate modes of excitation. For the *even mode*, where $V_{g2} = V_{g3} = 2V_0$, and the *odd mode*, where $V_{g2} = -V_{g3} = 2V_0$.

Then by superposition of these two modes, we have an excitation of $V_{g2} = 4$, $V_{g3} = 0$, from which we can find the S parameters of the network. We can work with these two circuits separately. If we look into port 2, we see an impedance of [11]:

$$Z_{in}^e = \frac{Z^2}{2} \quad (1)$$

The transmission line behave like a quarter-wave transformer. If $Z_0 = \sqrt{2}$, port 2 will be matched for even mode excitation. The $r/2$ resistor is not important in this case, since one end is open-circuited. Then, we find V_1^e from the transmission line equations.

$$V_2^e = V(-(\lambda/4)) = j V^+(1 - \rho) = V_0 \quad (2)$$

$$V_1^e = V(0) = V^+(1 - \rho) \quad (3)$$

$$\rho = \frac{2 - \sqrt{2}}{2 + \sqrt{2}} \quad (4)$$

$$V_1^e = -j V_0 \sqrt{2} \quad (5)$$

In the case of the *odd-mode* excitation, $V_{g2} = -V_{g3} = 2V_0$ and $V_2^0 = -V_3^0$, and there is a voltage null along the circuit. So, we can separate this circuit by grounding it at two points on its midplane. Looking into port 2, we see an impedance of $r/2$, since the parallel-connected transmission line is $\lambda/4$ long shorted at port 1, and so looks like an open circuit at port 2.

Port 2 will be matched for odd mode excitation if we select $r = 2$. Finally, we must find the input impedance at port 1 of the Wilkinson divider when ports 2 and 3 are terminated in matched loads.

The input impedance is [11]:

$$Z_{in}^0 = \frac{1}{2} (\sqrt{2})^2 = 1 \text{ (matched)} \quad (6)$$

$$V_2^0 = V_0 \quad (7)$$

$$V_1^0 = V_0 \text{ (virtual ground)} \quad (8)$$

When ports 2 and 3 are terminated with matched loads, there is no current flow through the normalized isolation resistor and it can be removed.

In conclusion, we can establish the following S parameters for the Wilkinson divider:

$$S_{11} = 0 \quad Z_{in} = 0 \text{ at port 1} \quad (9)$$

$$S_{22} = S_{33} = 0 \text{ output matched for even/odd modes} \quad (10)$$

$$S_{12} = S_{21} = \frac{V_1^e + V_1^e}{V_2^e + V_2^e} = -j / \sqrt{2} \quad \text{symmetry due to reciprocity} \quad (11)$$

$$S_{13} = S_{31} = -j / \sqrt{2} \quad \text{symmetry of ports 2 and 3} \quad (12)$$

$$S_{23} = S_{32} = 0 \quad \text{due to short or open at bisection} \quad (13)$$

The S-matrix can be written as [21]:

$$[S] = \frac{-1}{\sqrt{2}} \begin{bmatrix} 0 & j & j \\ j & 0 & 0 \\ j & 0 & 0 \end{bmatrix}$$

When the divider is working at port 1 and the outputs are matched, no power is dissipated in the resistor. Thus, the divider is lossless when the outputs are matched, only reflected power from ports 2 or 3 is dissipated in the resistance. The frequency response of the equal-split Wilkinson divider is shown in Figure 4.15 below. The figures are shown over the band from 0.5 to 1 GHz [21].

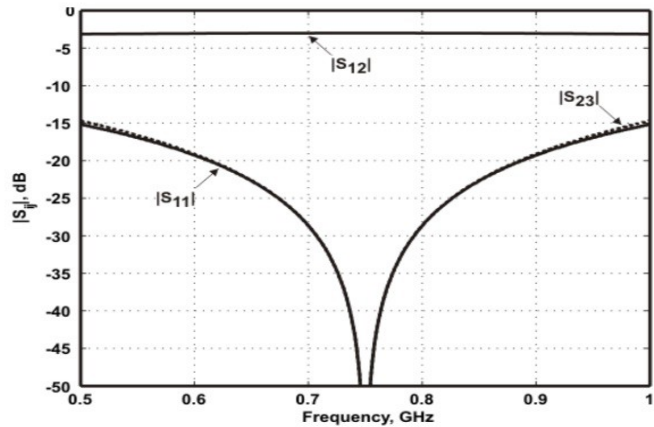


Figure 4.15 Frequency response of an equal-split Wilkinson power divider.

4.5 SCHEMATIC LEVEL DESIGN in ADS

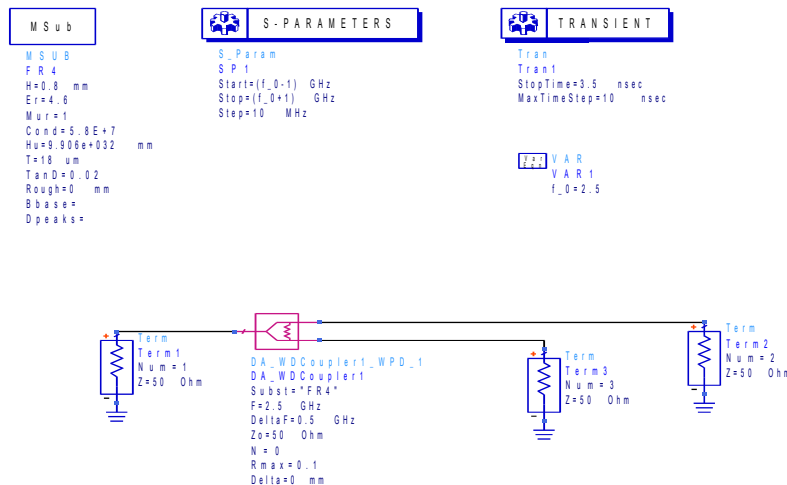


Figure 4.16 Smart component with S-parameter and Transient parameter simulation set-up.

The circuit will be simulated for both transient behaviour and S-parameters estimation. All the parameters are the same as in the Branch Coupler design. If you use Term1 as the input and Term2 and Term3 as two outputs, you will have a power splitter. On the other hand, if you use Term2 and Term3 as two inputs and Term1 as the output, you will have a power combiner. We chose the first one mentioned. It will be working for the specified central frequency, in this case as before it was said, 2.5 GHz.

It has been created a variable called f_0 for this value. We will be using a step size of 10 MHz. The time-domain simulation has a StopTime of 3.5 nsec, and a maximum step-size of 10 nsec. The two outputs Term2 and Term3 are terminated in two equal 50Ω loads. The substrate FR4 was defined with a TanD of 0.02, it has relative permittivity (ϵ_r) of 4.6, it has 0 mm of roughness and a relative permeability (μ_r) of 1 (Nonmagnetic material).

The frequency response will be optimized and the time-domain will be illustrated. It will be design and optimize using a $K = 1$. The K-parameter of the power divider represents the ratio of the power delivered to Port 3 to the power delivered to Port 2.

4.6 LAYOUT LEVEL DESIGN in ADS

In the layout generation, I removed the shunt resistor automatically placed by ADS and replace it with two ports, “P4” and “P5”.

I modified the ports “P4” and “P5” calibration type, from “TML” to “TML (zero length)”.

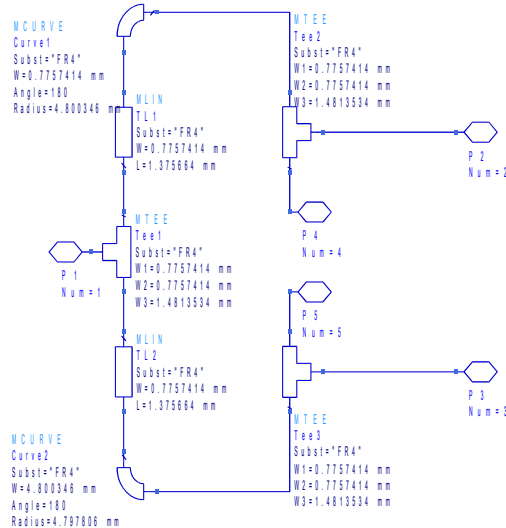


Figure 4.17 Schematic of the microstrip Wilkinson power divider.

4.7 S - PARAMETERS

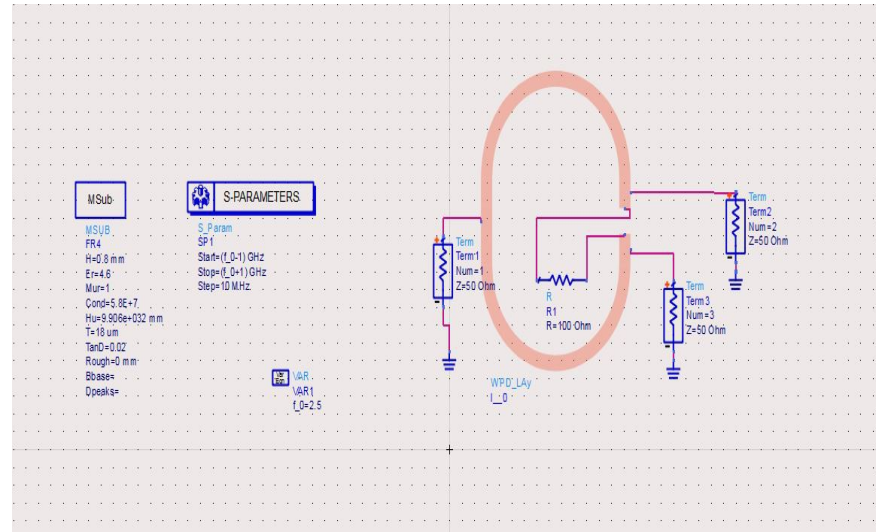
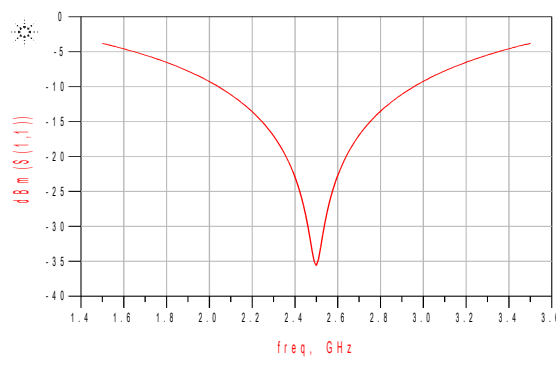
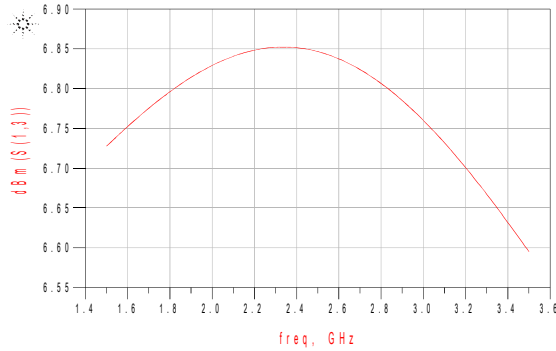


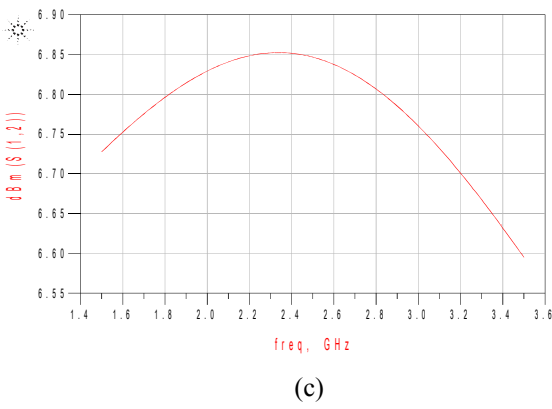
Figure 4.18 The Wilkinson power divider as a layout component S-parameters simulation set-up. The results were optimize f_o the frequency given. In this case, 2.5 GHz.



(a)



(b)



(c)

Figure 4.19 Simulated S-parameters of the Wilkinson Power Divider. (a) S(1,1), (b) S(1,2) and (c) S(1,3) parameter.

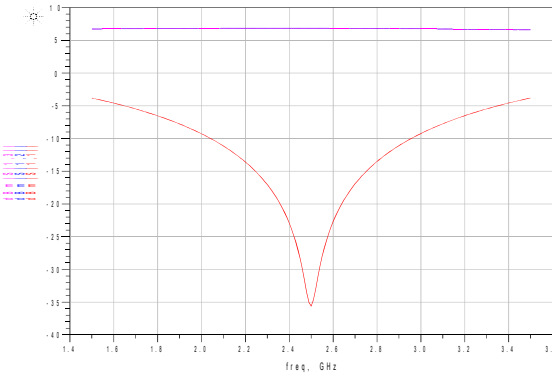


Figure 4.20 Simulated S-parameters. S(1,1) ,S(1,2) and S(1,3) parameter.

As it is shown in Figure 4.20, Is the typical output expected from a Wilkinson power divider.

The S-parameters plotted show the frequency response of the Wilkinson power divider. Good input impedance matching characteristics are observed and the coupled power at each output port is about -3 dB around 2.5 GHz.

S(1,2) and S(1,3) has a very high near design frequency (almost coincided). Both of them are almost -3 dB and are essentially identical, demonstrating the reciprocal nature of the Wilkinson.

$S(1,1)$ is low near the design frequency. It has a very small reflexion. The frequency at which the isolation reaches a maximum value (-36 dB) is approximately 2.5 GHz. Furthermore, the divider provides good isolation (>20 dB) between 2.3 GHz and 2.55 GHz.

The overall bandwidth can be determinated by looking at the bandwidth of the return losses, the amplitude balance, and the isolation (Figure 4.21).

The elements $S(2,3)$ and $S(3,2)$ are associated with the isolation between the output ports. These correspond to signals entering port two and exiting port three and other way round. When the magnitudes of these elements are small, high isolation is achieved between the ports [1-3].

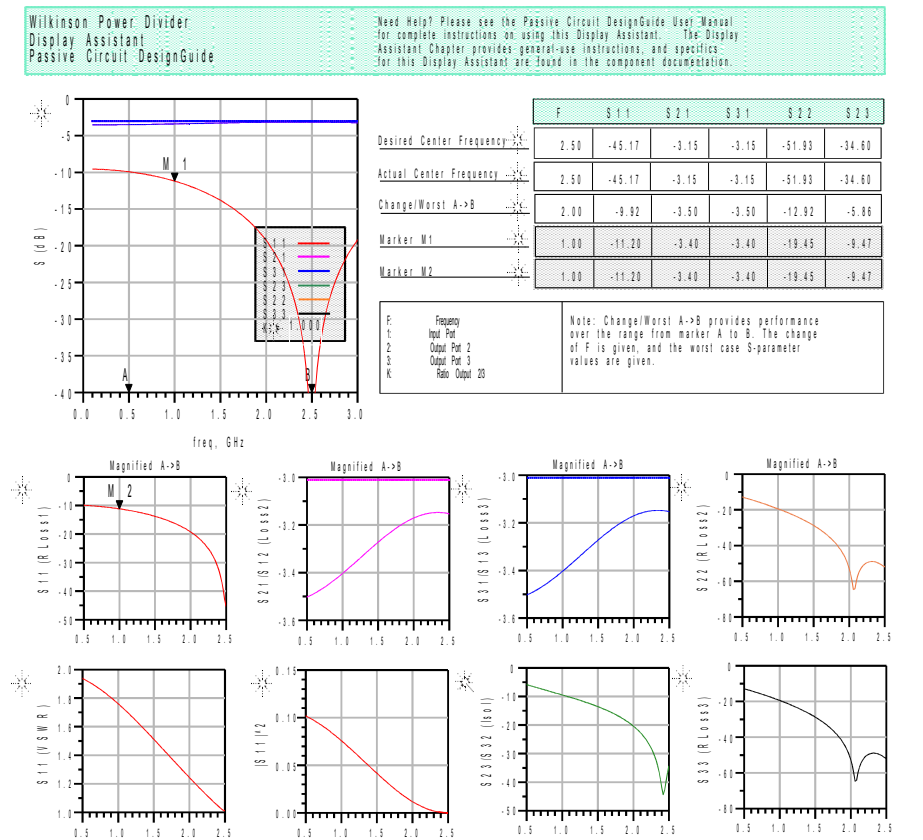


Figure 4.21 Optimized parameters.

4.8 LAYOUT LEVEL. TRANSIENT SIMULATION

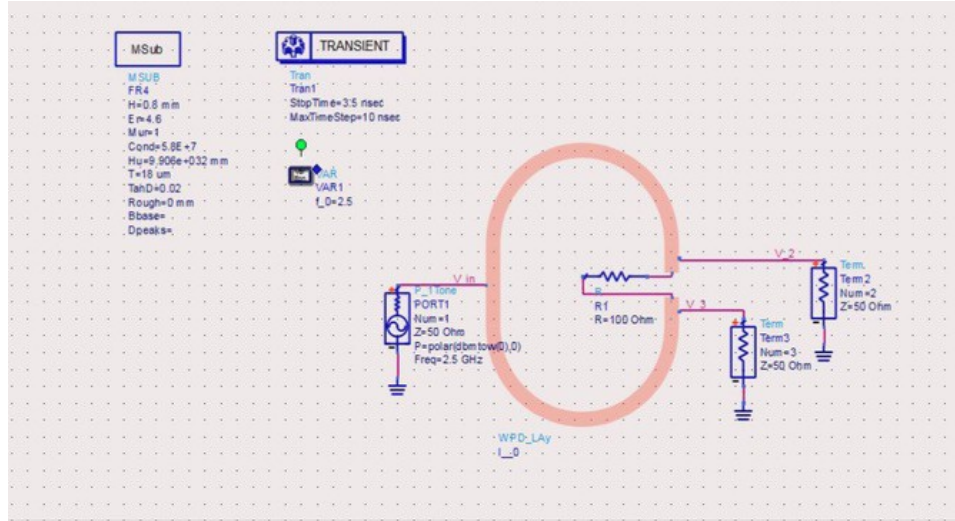
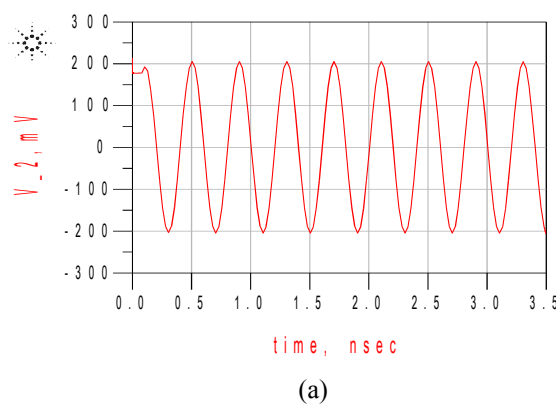


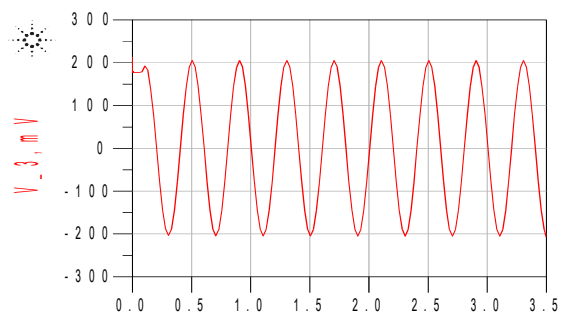
Figure 4.22 The Wilkinson power divider as a layout component and transient simulation set-up.

We use a $R_1 = 100 \Omega$ between V_2 and V_3 . As it was explained before, transient simulations can only be performed when you apply a time-domain signal. Thus, you need a P_1Tone source at port1 and labels on the output termination wires to display them after simulation. It was chosen a $Z = 50 \Omega$ and the frequency given 2.5 GHz. All the outputs were labelled clockwise to respect the port convention for BLCs as illustrated in Figure 4.21.

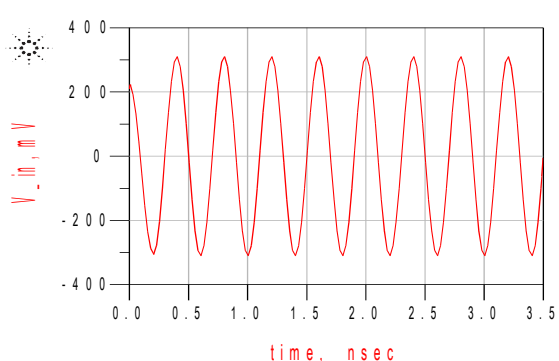
4.9 TRANSIENT SIMULATION. SIMULATION RESULTS



(a)



(b)



(c)

Figure 4.23 Transient simulations (a) $V_{2, \text{mV}}$, (b) $V_{3, \text{mV}}$, and (c) $V_{\text{in}, \text{mV}}$.

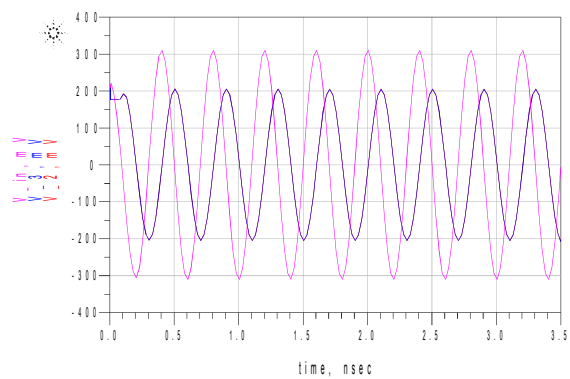


Figure 4.24 Transient simulations. $V_{2, \text{mV}}$, $V_{3, \text{mV}}$, $V_{\text{in}, \text{mV}}$.

ADVANTAGES OF USING A WILKINSON POWER:

Simplicity: The Wilkinson power divider is really simple and can easily be done using printed components on a printed circuit board. It is also possible to use lumped inductor and capacitor elements, but this complicates the overall design.

Cost: When the Wilkinson power divider is done using printed circuit elements, the cost is very low.

Loss: If perfect components were used, the Wilkinson splitter divider would not introduce any additional loss between the different ports. In addition to this, the real components used for the Wilkinson splitter can be very low loss.

Isolation: The Wilkinson divider provides a high degree of isolation between the output ports.

DISADVANTAGES OF USING A WILKINSON POWER:

Frequency response: As the Wilkinson splitter is based around the use of quarter wave transmission lines, it has a limited bandwidth.

5. MULTI-PORT RECEIVER DESIGN

In this chapter the design of the multi-port correlator, the multi-port receiver and the simulation in ADS are presented.

5.1 LAYOUT LEVEL DESIGN in ADS

In the layout generation we combine three branch line couplers with one Wilkinson power divider and create a six-port. We have two inputs and 6 outputs. We connected the Wilkinson power divider as the main input and the 6 outputs were made by the same three branch couplers. Thus, we linked them with MLIN (Microstrip Line). It consists of a conducting strip and MCORN (90° Microstrip Bend). We also added a MLIN in the Port “P1”. MLIN (Microstrip Line) was built on an FR4 (standard PCB) substrate. The PCB substrate was defined as it was said before (Figure 4.3). FR4 is a popular thermoset plastic laminate grade with good strength to weight ratios. Actually, It is commonly used as an electrical insulator considerable mechanical strength. The material is known to retain its high mechanical values and electrical insulating qualities in both dry and humid conditions.

The schematic of the multi-port receiver it is shown in Figure 5.1.

5.2 SCHOTTKY BARRIER DIODE

The HSMS-286x is a family of biased detector diodes have been designed and optimised for use from 915 MHz to 5.8 GHz. They are ideal for RF/ID and RF tag applications as well as large signal detection, modulation and RF to DC conversion. Commonly used for high performance biased detectors. Below we can see the characteristics of the diode we are going to use (Figure 5.2). They are different configurations available.

This decides the dynamic range of the diode detectors and hence the dynamic range of the whole receiver system.

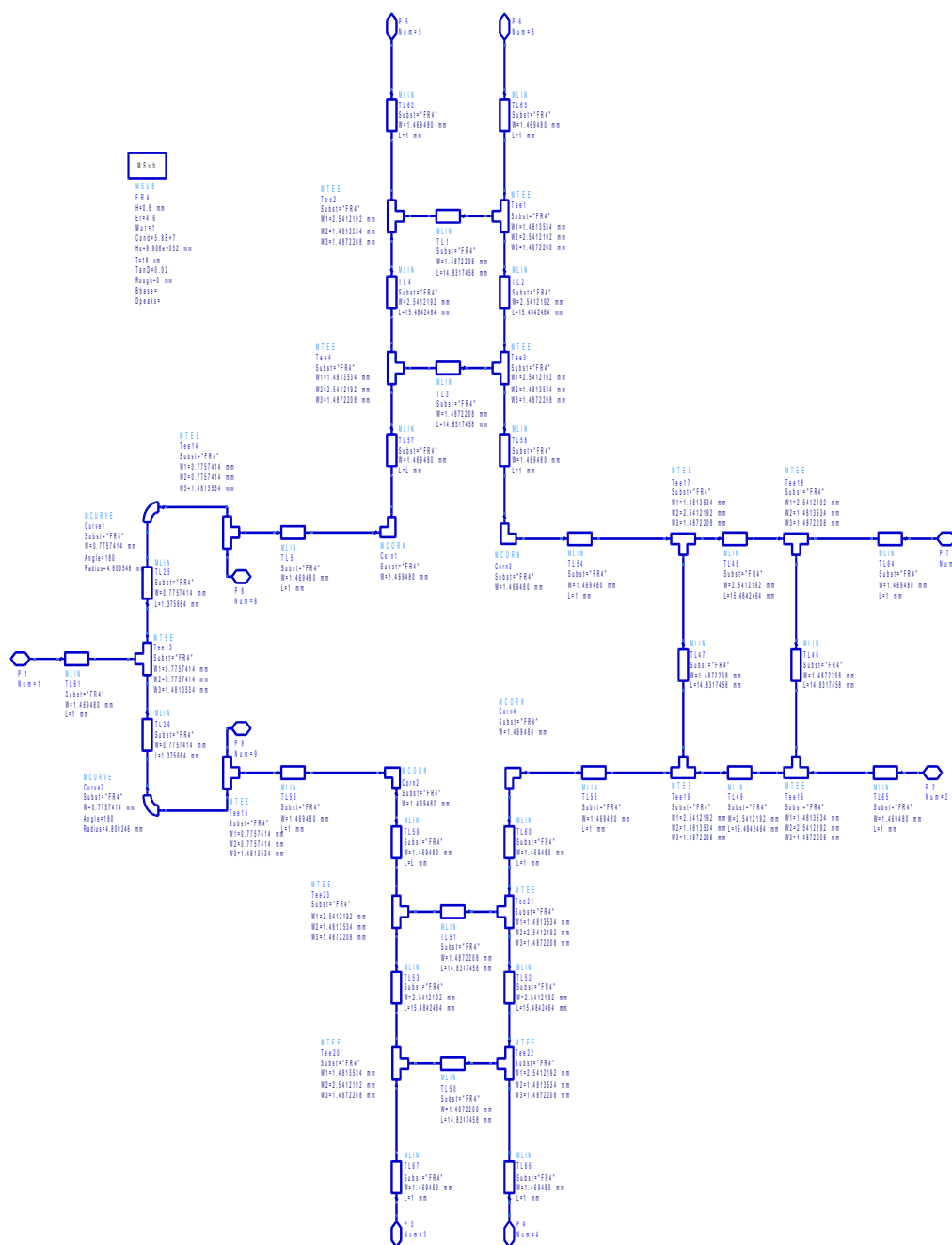


Figure 5.1 Schematic of the Multi-Port heterodyne receiver.

```

Diode Model
HSMS286x
Is=5E-8    Bv=7    Vjsw=
Rg=6      Ibv=1E-5   Fsw=
Gleak=    Nbv=     AllowScaling=0
N=1.08    Ibv=     Tl0nm=
Tf=0      Nbvle=   Trise=
Cd=       Kf=      Xl=2
Cjo=0.18E-12 Af=    Eg=0.68
Vj=1.8    Ffa=    AllParams=<Invalid form: "AllParams">
M=0.5    Isw=    Msw=
Fz=1.5    Rsw=    Lmax=
Imax=    Gleaksw=  Imell=
Imell=    Ng=     Isr=
Isr=     Ikg=     Njw=
Njw=     Cjsw=    If=
If=      Msw=

```

Figure 5.2 Diode HSMS286x definition.

They are used for low cost, high volume designs in two kind of applications. This diode is used with DC bias at frequencies up to 1.5 GHz. In our case, 2.5 GHz. For lower frequencies the use of this diode should be considered.

5.3 SCHOTTKY BARRIER DIODE CHARACTERISTICS

A Schottky barrier diode chip consists of a metal-semiconductor barrier formed by deposition of a metal layer on a semiconductor. It is a semiconductor diode with a low forward voltage drop and a very fast switching action. The current-voltage characteristic of a Schottky barrier diode at room temperature is described by the following equation [21]:

$$I = I_s (\exp(\frac{V - IR_s}{0.026}) - 1)$$

On a semi-log plot the current graph will be a straight line with inverse slope of $2.3 \times 0.026 = 0.060$ volts per cycle. All Schottky diode curves have the same slope, but not necessarily the same value of current for a given voltage. This is determined by the saturation current, I_s , and is related to the barrier height of the diode.

Through the choice of p-type or n-type silicon, and the selection of metal, it can tell the characteristics of a Schottky diode. Generally, only low barrier height diodes are realized on p-type silicon. The choice of the combination of the metal and semiconductor determines the forward voltage of the diode. Both n-type and p-type

semiconductors can develop Schottky barriers. However, the p-type typically has a much lower forward voltage. As the reverse leakage current increases dramatically with lowering the forward voltage, it can not be too low, so the usually employed range is about 0.5 – 0.7 V [24].

In ADS, we worked with the diode HSMS286x in ADS. In Fig.5.3, we can see the Schematic and in Figure 5.4 its symbol from the library.

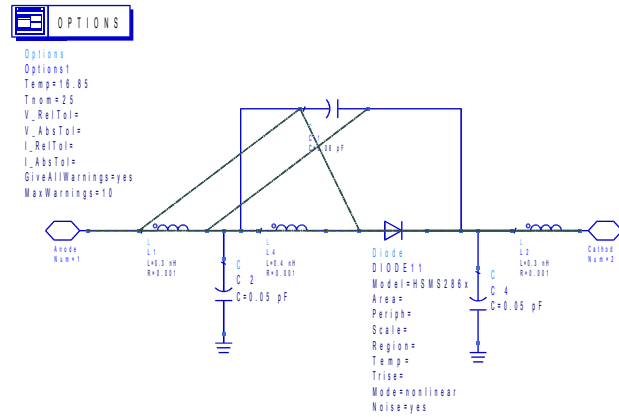


Figure 5.3 Schematic of diode HSMS286x.

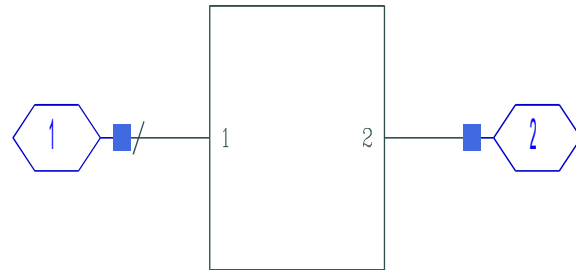


Figure 5.4 Symbol of diode HSMS286x.

In Figure 5.5 we can see an ideal multi-port receiver. Later, it was replaced the PwrSplit2 and 3 Hybrid90 for three branch coupler and one Wilkinson power divider as it is shown below in Figure 5.6.

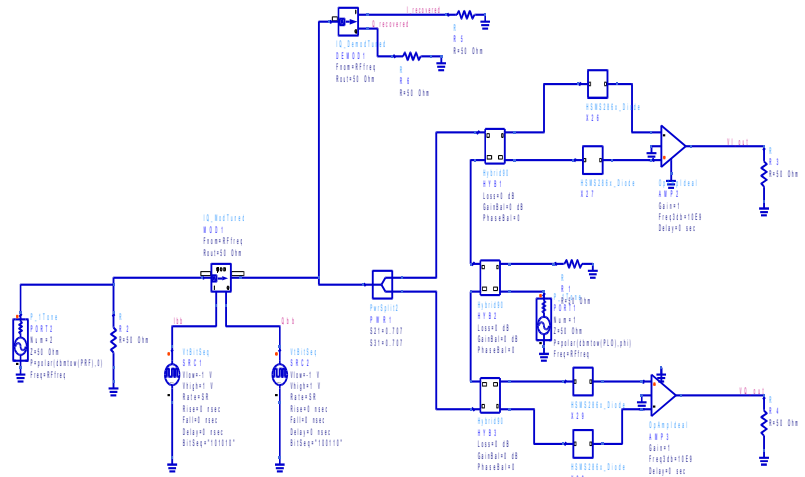


Figure 5.5 Simulation set-up of the ideal Multi-Port receiver.

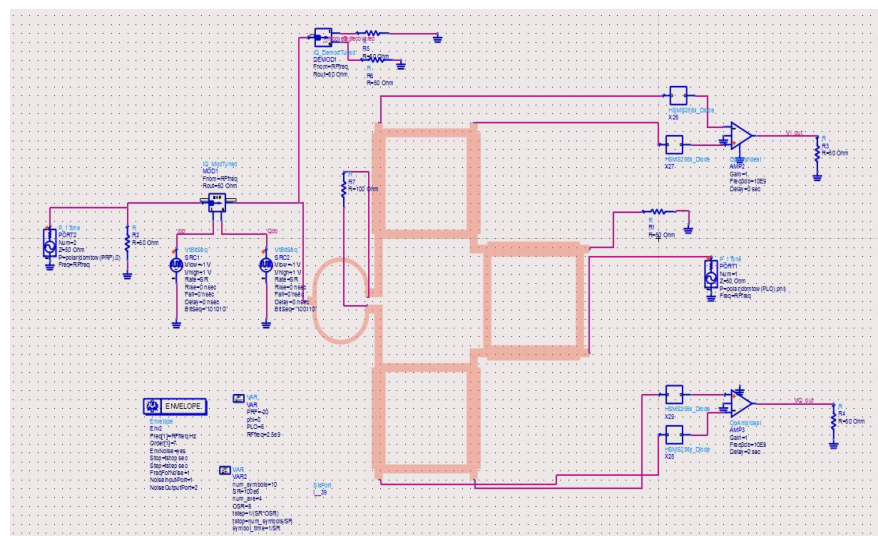
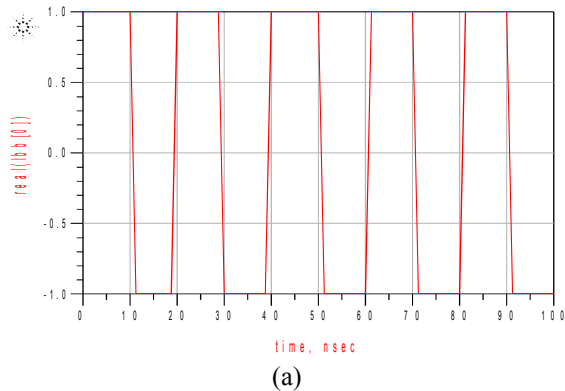
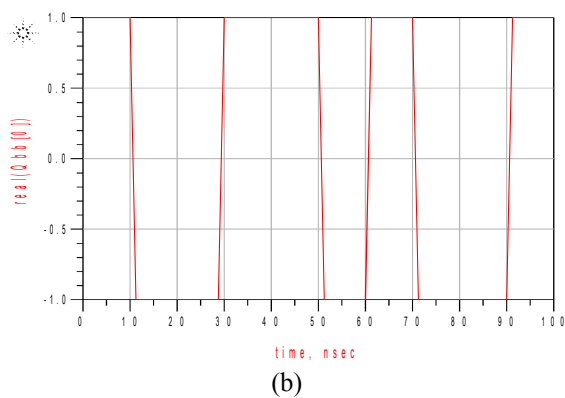


Figure 5.6 Simulation set-up of the Multi-Port receiver.

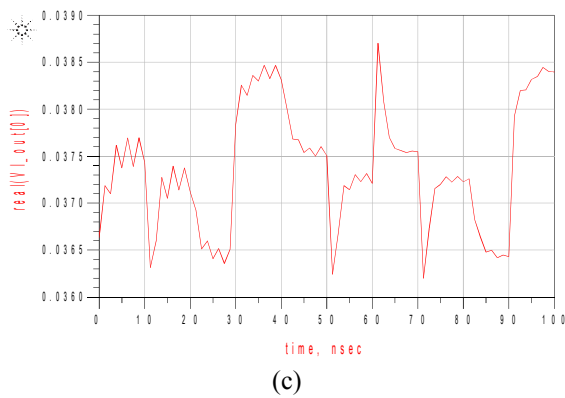
5.4 SIMULATION RESULTS



(a)



(b)



(c)

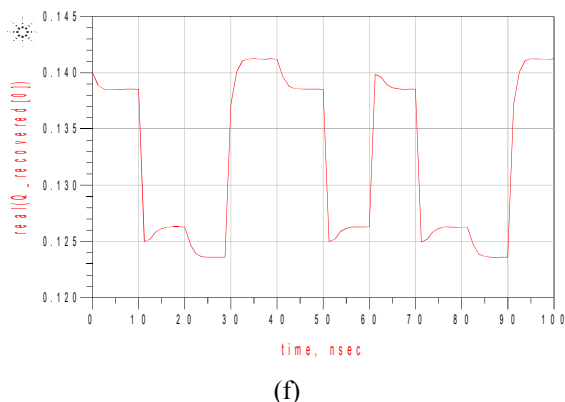
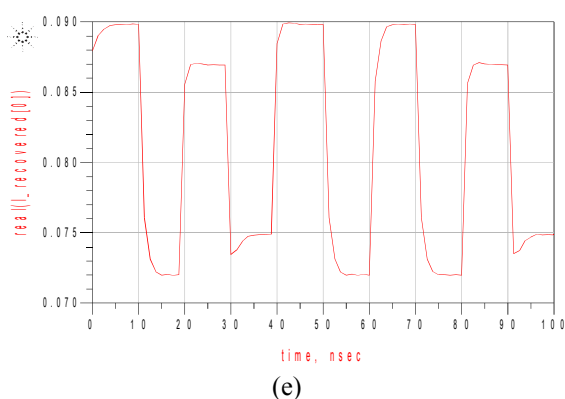
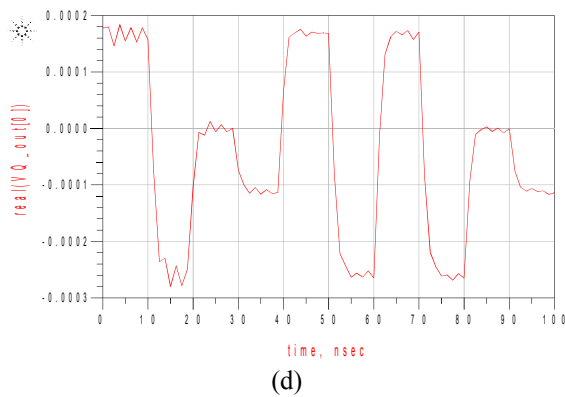


Figure 5.7 Demodulation results.

6. APPLICATION OF MULTI-PORT RECEIVER

In this chapter the use of the multi-port receiver for microwave sensor for detection of vital signs is analyzed.

6.1 WIRELESS COMMUNICATIONS SYSTEMS

Wireless communications is, the fastest growing segment of the communications industry. Cellular systems have experienced exponential growth over the last decade and there are currently around two billion users worldwide. Many new applications, including wireless sensor networks, automated highways and factories, appliances and remote telemedice, are emerging from reseach today. Many technical challenges remain in designing robust wireless networks that deliver the performance necessary to support emerging applications [25], such as, radar sensor for respiration and heartbeat monitoring.

The vision of wireless communications supporting information exchange between people and devices is the communications frontier of the next few decades, and much of it already exists in some form. Wireless networks will connect laptop, and desktop computers anywhere within an office building. Wireless sensors have an enormous range of both commercial and military applications. In our case of study, we will focus on the communication between a device and a patient in which the radiated signal from the device, it mainly reflected at the patient's upper skin layer.

The exponential growth of cellular telephone use and wireless Internet access have led to great optimism about wireless technology in general. Obviously not all wireless applications will flourish. While many wireless systems and companies have enjoyed spectacular success, ther have been many failures along the way. In fact, is it impossible to predict what wireless failures and triumphs lie on the horizon. Moreover, there must be sufficient flexibility and creativity among both engineers and regulators to allow for accidental successes. The current and emerging wireless systems of today and the vision of applications that wireless can enable insure a bright future for wireless technology

[3]. Design of wireless networks differs fundamentally from wired network design due to the nature of the wireless channel. This channel is an unpredictable and difficult communications medium. A global system operating in a given frequency (our case 2.5 GHz) band must obey the restrictions for that band set forth by the corresponding regulatory body. At frequencies around several Gigahertz wireless radio components with reasonable size, power consumption, and cost are available. However, the spectrum in this frequency range is extremely crowded .

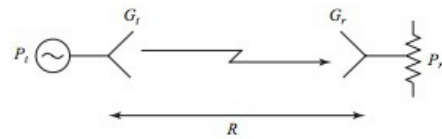


Figure 6.1 A basic radio system [26].

6.2 RADAR SYSTEMS

One of the most prevalent applications of microwave technology is Radio Detection and Ranging. In its basic operation, a transmitter sends out a signal which is partly reflected by a distant target, and then detected by a sensitive receiver. The distance to the target is determinated by the time required for the signal to travel to the target and back, and the radial velocity of the target is related to the Doppler shift of the return signal.

Early radar work in the United States and Britain began in the 1930s using very high frequency (VHF) sources. A major breakthrough occurred in the early 1940s with the British invention of the magnetron as a reliable source of high-power microwaves. Higher frequencies allowed the use of reasonably sized antennas with high gain, allowing mechanical tracking of targets with good angular resolution [12].

Most radars are of the monostatic type, but in some applications the target is illuminated by a separate transmit antenna. Sometimes separate antennas are used to achieve the necessary isolation between transmitter and receiver. It is assumed that the target is in the main beam direction of the antenna. The target will scatter the incident

power in various directions; the ratio of the scattered power in a given direction to the incident power density is defined as the radar cross section, σ , of the target.

$$\sigma = \frac{P_s}{S_t}$$

Where P_s is the total power scattered by the target.

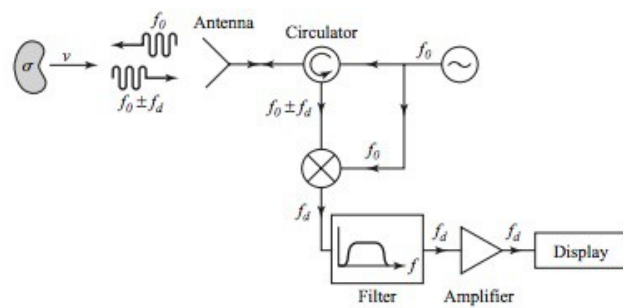


Figure 6.2 Doppler radar system [10].

DOPPLER RADAR

The Doppler effect is observed whenever the source of waves is moving with respect to an observer. The Doppler effect can be described as the effect produced by a moving source of waves in which there is an apparent upward shift in frequency for observers towards whom the source is approaching and an apparent downward shift in frequency for observers from whom the source is receding. It is important to note that the effect does not result because of an actual change in the frequency of the source. The Doppler effect can be observed for any type of wave - water wave, sound wave, light wave, etc. We are most familiar with the Doppler effect because of our experiences with sound waves.

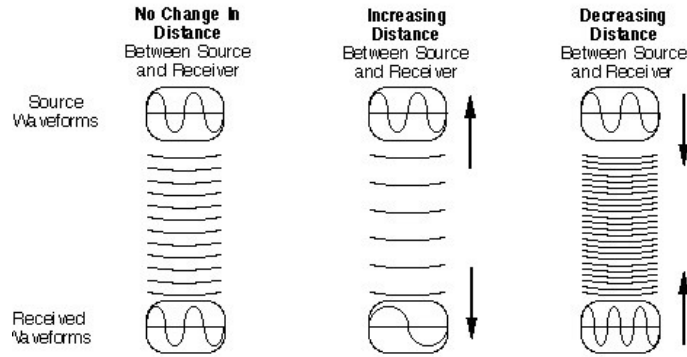


Figure 6.3 Doppler Effects [6].

The above formula assumes that the source is either directly approaching or receding from the observer. When the distance between the source and receiver of electromagnetic waves remains constant, the frequency waves is the same in both places. When the distance between the source and receiver of electromagnetic waves is increasing, the frequency of the received wave forms is lower than the frequency of the source wave form. When the distance is decreasing, the frequency of the received wave form will be higher than the source wave form.

$$\Delta f = \frac{\Delta v}{c} f_0$$

Where, $\Delta f = f - f_0$

$\Delta v = V_r - V_s$ is the velocity of the receiver relative to the source: it is positive when the source and the receiver are moving towards each other.

MULTI-PORT MICROWAVE SENSOR

The radar system used in this application uses frequency modulated continuous waves that are transmitted into free air by the use of an antenna. The radiated signal will be reflected in the patient's upper skin layer, they are directed back to the system and they are being received through the same antenna, that they have been sent out. This

wave is being processed by a multi-port correlator (it was explained before) and power detectors. This multiport system works as an interferometer, its output signals are linear combinations of phase shifted input signals [5]. By using the circuit design (Fig. 5.6) and devices connected to the output ports, this circuit can provide specific parameters of microwave/millimeter-wave frequencies. As a result, the information can be extracted by the wave it was previously sent.

Its highlights are, excellent phase discrimination, trivial signal processing, low circuit complexity, broadband operation, high data rate and cost. Multi-port radarmodule aiming at a reliable high-integration of all subcomponents such as antenna, Multi-port front-end, baseband circuitry, and digital signal processing in one single package [4].

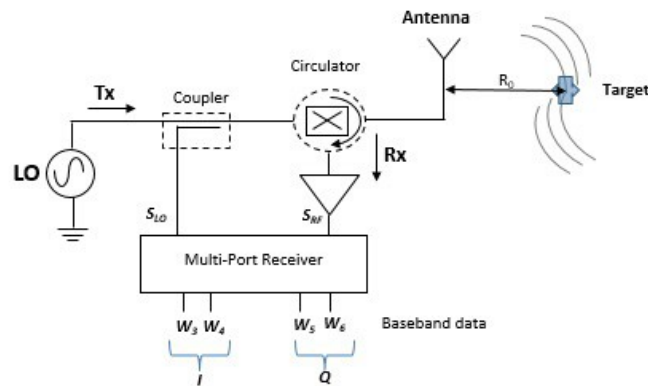


Figure 6.4 Multi-port microwave sensor with direct conversion architecture.

As it was shown in Chapter 2, the heartbeat and breathing activities affect the phase of the reflected signal, which is compared with the reference signal source in the radar device. The radiated signal will mainly be reflected at the patient's upper skin layer then, the patient's respiration will result in a periodic movement of the "target" in the range of several millimeters. Finally, the heartbeat will be superimposed to this movement and it is in sub-millimeter range.

In Figure 6.4, a continuous wave is sent from the target via the antenna. This signal travels the distance R and scatters on the target at the distance R . We can model this by a small change of R with:

$$R(t) = R_0 + r(t) \quad \text{Where, } R_0 = \text{constant}$$

This signal will travel back the distance that depends on time $R(t)$, a phase delay depending on $R(t)$ can be detected:

$$\Phi(t) = -\frac{4\pi}{\lambda} R(t) = \frac{4\pi}{\lambda} R_0 - \frac{4\pi}{\lambda} r(t) = \Phi_0 + \Phi(t)$$

Ideally the two signals can be written:

$$A_{LO}(t) = A_{LO} \cos(\omega_{LO} t)$$

$$A_{RF}(t) = A_{RF} \cos(\omega_{LO} t + \Phi(t) + \Phi_e)$$

Where Φ_e is a static phase delay due to the delay. Through the systems, R_0 is a constant and $\Phi(t)$ is the phase modulated by the variation.

In a direct conversion receiver architecture, the baseband signal is obtained as follows:

$$A_{BB}(t) = A_{LO} A_{RF} = A_{LO} \cos(\omega_{LO} t + \Phi_{LO}) = A_{RF} \cos(\omega_{LO} t + \Phi(t) + \Phi_e) =$$

$$= \frac{1}{2} A_{LO} A_{RF} [\cos(2\omega_{LO} + \Phi(t) + \Phi_e + \Phi_{LO}) + \cos(\Phi(t) + \Phi_e - \Phi_{LO})]$$

Then, after LPF, we obtain:

$$A_{BB}(t) = A_{BB} \cos(\Phi(t) + \Delta\Phi)$$

For certain values of $\Delta\Phi$, $A_{BB}(t) = A_{BB} \cos(\Phi(t) + \Delta\Phi)$ anything is obtained, they are called NULL-POINTS. A Second non-ideality is the presence of DC-Terms is $A_{BB}(t)$, called DC-offsets.

To increase the probability of detections, the Doppler radar can be enhanced with a complex incoming signal in form of I and Q baseband signals.

$$A_{BB}^I(t) = A_{BB} \cos(\Phi(t) + \Delta\Phi)$$

$$A_{BB}^Q(t) = A_{BB} \cos(\Phi(t) + \Delta\Phi)$$

If the total static error $\Delta\Phi$ is: $\Delta\Phi = (2n + 1)\pi/2$

The variation in terms of the phase due to the target vibrations can be expressed in terms of frequency as follows:

$$\omega = \frac{d\Phi}{dt} = \frac{d}{dt} \left[-\frac{4\pi r(t)}{\lambda} + \Delta\Phi \right]$$

$$\omega = -4\pi \frac{dr(t)}{dt}$$

That illustrates that the spectrum of the demodulation only one frequency can be detected if $\Delta\Phi$ is constrict.

DOPPLER RADAR SIMULATIONS

A Doppler radar is a specialized radar that makes use of the Doppler Effect to produce velocity data about objects at a distance. It does this by beaming a microwave signal towards a desired target and listening for its reflection, then analyzing how the frequency of the returned signal has been altered by the object's motion. This variation gives direct and highly accurate measurements of the radial component of a target's velocity relative to the radar (Figure 6.5).

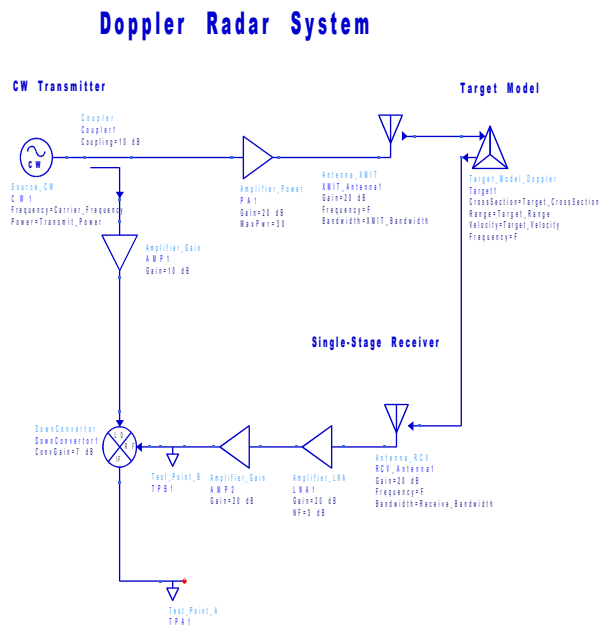


Figure 6.5 Doppler radar implements in ADS – behavioral level.

It has only 1 mixe, due to the property of Homodyne Architecture. The Doppler radar transmits a signal which splits at PS1 and PS2. PS1 signal have a 90 degrees phase delay from PS2. PS1 and PS2 signals merged together to form the received signal which have a frequency value similar to the transmitter signal frequency (Figure 6.6).

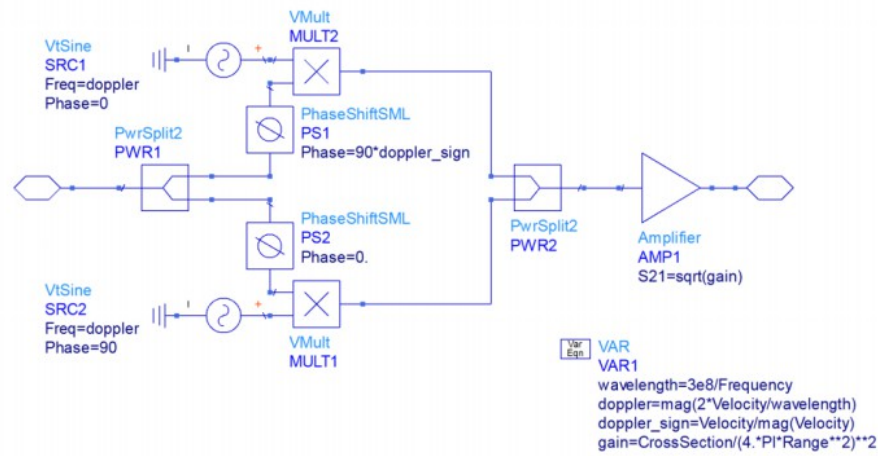
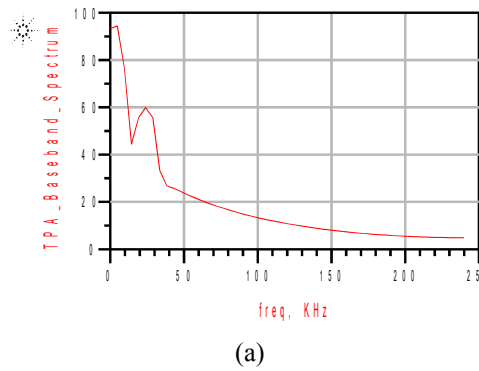
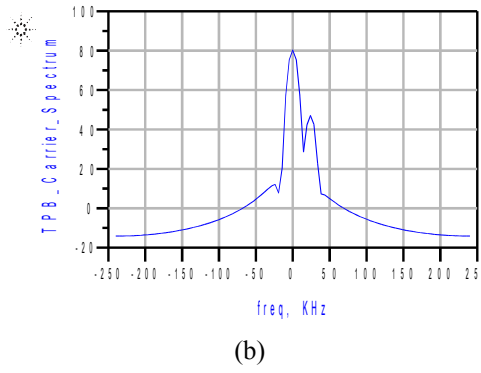


Figure 6.6 Target model in ADS for a Doppler radar.

The maximum of the step parameter is $2xfo$. In order to obtain the same signal the received as the transmitted signal we use the Nyquist theorem and it has to be fulfilled. If there is 2 signal, the minimum signal have to be equal or greater than $2xfo$, so that the signals do not overlap and the original transmitted signal can be recovered.





(b)

Figure 6.7 Simulation Results. (a) TPA_Baseband_Spectrum, (b) TPB_Carrier_Spectrum.

The diagram on Figure 6.7 (a) show a baseband signal and Figure 6.7 (b) show a pure analog signal. Both of them, TPA and TPB signal, have the same frequency, $f_d = 24 \text{ KHz}$ at their peaks and they have the same $f_o = 0$. The difference is that TPA has a spectrum of 60 dBm while TPB has a spectrum of 47 dBm. TPA has a higher amplitude because it passes through a mixer which gives it a slightly higher amplitude as compared to TPB.

Both signals have the same frequency but at different peaks. There is lower isolation thus its receiver have higher amplitude as the signal is not fully isolated at the circulator. As the object moves towards the antenna, the receiver is delayed due to $f_o - f_d$.

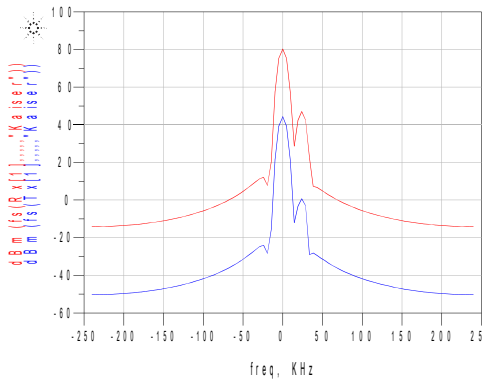


Figure 6.8 Simulation ADS for a Doppler-radar.

Variable gain amplifier (VGA) amplifies the received signal which gives a higher amplitude as compared to the transmitted signal (Figure 6.9).

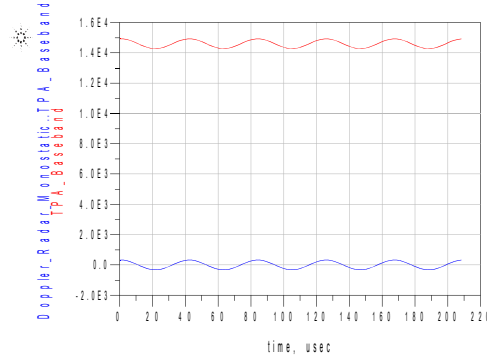


Figure 6.9 Simulation ADS for a Doppler-radar.

7. CONCLUSIONS

Based on the well-known background of the multi-port technique, the demodulation results demonstrate the validity of the proposed heterodyne architecture for the multi-port radar Sensor.

If the difference between the carrier and the local oscillator is not exactly equal to IF, the demodulated constellation turns clockwise or anti-clockwise, depending on the sign of this difference. The dynamic range has been achieved thanks to the use of biased detector diodes.

The results reveal the basic theory on multi-port receivers (multi-port architecture has been implemented for 2.5 GHz). It has been shown that the sixth port offers the possibility of realizing a broadband multi-mode/band receiver. The comparison to conventional receiver architectures shows that the multi-port receiver is an interesting alternative to existing mixer based architectures especially in millimeter and sub-millimeter wave range.

It has been demonstrated that the multi-port is not a mystic component that can get six power measurements from which the in-phase and quadrature-phase components of the incoming bandpass signal can be calculated in an obscure way. There is rather an ordinary frequency conversion that takes place.

It was demonstrated empirically and quantitatively the multi-band behaviour of the multi-port architecture, and the capability of performing high data rates. The main advantage of the multi-port architecture is its extremely large bandwidth, which involves multi-band and multi-mode capabilities. However, an important problem is the large dimensions of the passive multi-port structure. As we know multi-port receiver system requires no external bias supply and the LO power requirement is comparable to the RF power level. These results may lead to consider the multi-port architecture as an alternative for mobile communication applications.

REFERENCES

- [1] <http://www.eucomed.be/medical-technology>
 - [2] <http://www.cypress.com/documentation/application-notes/an62651-psoc-3-psoc-5-blood-pressure-monitor-analog-front-end>
 - [3] <http://searchmobilecomputing.techtarget.com/definition/wireless>
 - [4] <http://www.hindawi.com/journals/jece/2014/194649/>
 - [5] <http://www.qrg.northwestern.edu/projects/vss/docs/communications/3-what-is-the-doppler-effect.htm>
 - [6] David M.Pozar, “Microwave Engineering”, Wiley, pp.664, 2005
 - [7] J. Li, R. G. Bosisio, and K. Wu, “Computer and measurement simulation of a new digital receiver operating directly at millimeter-wave frequencies,” IEEE Trans. Microw. Theory Tech., vol. 43, no. 12, pp. 2766–2772, Dec. 1995.
 - [8] S. B. Cohn and N. P. Weinhause, “An automatic microwave phase measurement system,” Microwave J., vol. 7, no. 2, pp. 49–56, Feb. 1964.
 - [9] Alexander Koelpin,Gabor Vinci,Benjamin Laemmle, and Robert Weigel,” The Enhanced Multi-Port Receiver: A new Concept for Simultaneous Data Reception and Direction of Arrival Detection” 2011 IEEE.
 - [10] David M.Pozar, “Microwave Engineering”, Wiley, pp.660-661, 2005
 - [11] De la Morena-Álvarez-Palencia, C., M. Burgos-García and J. Gismero-Menoyo, “Contribution of LTCC technology to the miniaturization of Six-Port networks”, European Microw. Conf., 659-662, Manchester, UK, Oct.2011.
 - [12] David M.Pozar, “Microwave Engineering”, Wiley, pp.647, 2005
 - [13] David M. Pozar, “Microwave Engineering”, 3rd ed. New York: Wiley, 2005, pp. .
-

-
- [14] Hentschel, “Six-Port communications receiver”, *IEEE Transactions on Microwave Theory and Techniques*, vol. 53, no. 3, march 2005 p. 1041.
- [15] J. Hyryläinen, L. Bogod, S. Kanagasmaa, H.-O. Scheck, and T. Ylämurto, “Six-Port direct conversion receiver” in 27th Eur. Microwave Conf. Exhibition, Jerusalem, Sep. 8–12, 1997, pp. 341–346.
- [16] Östh Joakim, “Study of Six-Port Modulators and Demodulators for High-Speed Data Communications”, pp.11, 2012.
- [17] <http://www.google.com/patents/WO2002067367A1?cl=en>
- [18] David M. Pozar, “Microwave Engineering”, 3rd ed. New York: Wiley, 2005, pp.318-323.
- [19] Östh Joakim, “Study of Six-Port Modulators and Demodulators for High-Speed Data Communications”, pp.11, 2012.
- [20] <http://ieeexplore.ieee.org/stamp/stamp.jsp?tp=&arnumber=1126617&isnumber=24930>
- [21] Y. Konishi, “Microwave Electronic Circuit Technology”, New York, New York: Marcel Dekker Inc. pp. 273-292, 1998.
- [22] David M.Pozar, “Microwave Engineering”, Wiley, pp.319-322, 2005.
- [23] J. Stiles, “The Wilkinson Power Divider,” University of Kansas, Dept. of EECS, 2009, <http://www.ittc.ku.edu/~jstiles/622/handouts/The%20Wilkinson%20Power%20Divider.pdf>, accessed 2012.
- [24] Nahin, Paul J. (2001), “The Science of Radio with Matlab and Electronics Workbench Demonstrations”(second ed.), New York: Springer-Verlag, AIP Press, ISBN0-387-95-150-4.
- [25] https://es.wikipedia.org/wiki/Diodo_Schottky
- [26] <http://wsl.stanford.edu/~andrea/Wireless/SampleChapters.pdf>

HSMS-286x Series

Surface Mount Microwave Schottky Detector Diodes



Data Sheet



Lead (Pb) Free
RoHS 6 fully
compliant

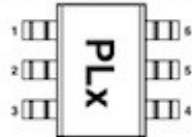


Description

Avago's HSMS-286x family of DC biased detector diodes have been designed and optimized for use from 915 MHz to 5.8 GHz. They are ideal for RF/ID and RFTag applications as well as large signal detection, modulation, RF to DC conversion or voltage doubling.

Available in various package configurations, this family of detector diodes provides low cost solutions to a wide variety of design problems. Avago's manufacturing techniques assure that when two or more diodes are mounted into a single surface mount package, they are taken from adjacent sites on the wafer, assuring the highest possible degree of match.

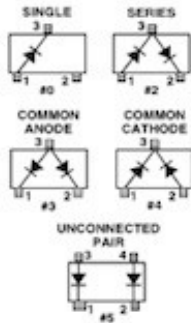
Pin Connections and Package Marking



Notes:

1. Package marking provides orientation and identification.
2. The first two characters are the package marking code.
The third character is the date code.

SOT-23/SOT-143 Package Lead Code Identification (top view)



UNCONNECTED PAIR

(3 leads)

1 2 3

4 5

6 7

8 9

10 11

12 13

14 15

16 17

18 19

20 21

22 23

24 25

26 27

28 29

30 31

32 33

34 35

36 37

38 39

40 41

42 43

44 45

46 47

48 49

50 51

52 53

54 55

56 57

58 59

60 61

62 63

64 65

66 67

68 69

70 71

72 73

74 75

76 77

78 79

80 81

82 83

84 85

86 87

88 89

90 91

92 93

94 95

96 97

98 99

100 101

102 103

104 105

106 107

108 109

110 111

112 113

114 115

116 117

118 119

120 121

122 123

124 125

126 127

128 129

130 131

132 133

134 135

136 137

138 139

140 141

142 143

144 145

146 147

148 149

150 151

152 153

154 155

156 157

158 159

160 161

162 163

164 165

166 167

168 169

170 171

172 173

174 175

176 177

178 179

180 181

182 183

184 185

186 187

188 189

190 191

192 193

194 195

196 197

198 199

200 201

202 203

204 205

206 207

208 209

210 211

212 213

214 215

216 217

218 219

220 221

222 223

224 225

226 227

228 229

230 231

232 233

234 235

236 237

238 239

240 241

242 243

244 245

246 247

248 249

250 251

252 253

254 255

256 257

258 259

260 261

262 263

264 265

266 267

268 269

270 271

272 273

274 275

276 277

278 279

280 281

282 283

284 285

286 287

288 289

290 291

292 293

294 295

296 297

298 299

300 301

302 303

304 305

306 307

308 309

310 311

312 313

314 315

316 317

318 319

320 321

322 323

324 325

326 327

328 329

330 331

332 333

334 335

336 337

338 339

340 341

342 343

344 345

346 347

348 349

350 351

352 353

354 355

356 357

358 359

360 361

362 363

364 365

366 367

368 369

370 371

372 373

374 375

376 377

378 379

380 381

382 383

384 385

386 387

388 389

390 391

392 393

394 395

396 397

398 399

400 401

402 403

404 405

406 407

408 409

410 411

412 413

414 415

416 417

418 419

420 421

422 423

424 425

426 427

428 429

430 431

432 433

434 435

436 437

438 439

440 441

442 443

444 445

446 447

448 449

450 451

452 453

454 455

456 457

458 459

460 461

462 463

464 465

466 467

468 469

470 471

472 473

474 475

476 477

478 479

480 481

482 483

484 485

486 487

488 489

490 491

492 493

494 495

496 497

498 499

500 501

502 503

504 505

506 507

508 509

510 511

512 513

514 515

<p

RF Electrical Specifications, $T_c = +25^\circ\text{C}$, Single Diode

Part Number HSMS-	Typical Tangential Sensitivity			Typical Voltage Sensitivity g			Typical Video Resistance RV (KΩ)
	915 MHz	2.45 GHz	5.8 GHz	915 MHz	2.45 GHz	5.8 GHz	
2860	-57	-56	-55	50	35	25	5.0
2862							
2863							
2864							
2865							
286B							
286C							
286E							
286F							
286K							
286L							
286P							
286R							
Test Conditions	Video Bandwidth = 2 MHz $I_b = 5 \mu\text{A}$			Power in = -40 dBm $R_L = 100 \text{ k}\Omega, I_b = 5 \mu\text{A}$			$I_b = 5 \mu\text{A}$

Absolute Maximum Ratings, $T_c = +25^\circ\text{C}$, Single Diode

Symbol	Parameter	Unit	Absolute Maximum ^[1]	
			SOT-23/143	SOT-323/363
P_{IV}	Peak Inverse Voltage	V	4.0	4.0
T_J	Junction Temperature	°C	150	150
T_{STG}	Storage Temperature	°C	-65 to 150	-65 to 150
T_{OP}	Operating Temperature	°C	-65 to 150	-65 to 150
θ_{JC}	Thermal Resistance ^[2]	°C/W	500	150

Notes:

1. Operation in excess of any one of these conditions may result in permanent damage to the device.
2. $T_c = +25^\circ\text{C}$, where T_c is defined to be the temperature at the package pins where contact is made to the circuit board.



Attention:
Observe precautions for handling electrostatic sensitive devices.

ESD Machine Model (Class A)

ESD Human Body Model (Class C)

Refer to Avago Application Note A004R: Electrostatic Discharge Damage and Control.

Typical Parameters, Single Diode

